



DESIGN METHODS FOR PILE GROUPS AND PILED RAFTS

METHODES DE CONCEPTION POUR GROUPES DE PIEUX ET RADIERES DE PIEUX

M.F. Randolph

Geomechanics Group
The University of Western Australia
Perth, Australia

SYNOPSIS: For many foundations, a shallow raft will provide adequate bearing capacity, but piles may be introduced in order to limit settlements to an acceptable level. In spite of this primary purpose of the piles, design methods still concentrate on providing adequate axial capacity from the piles to carry the structural load, and estimation of settlement is generally treated as a secondary issue. There is a need to reverse these priorities, and to develop new analytical methods that allow simple estimation of the stiffness of pile foundations systems, and hence permit design studies to focus on settlement issues rather than capacity. With this aim, the paper reviews analytical approaches for pile groups and piled raft foundations, and discusses appropriate choice of soil modulus for pile problems. The manner in which the non-linear stress-strain response of soil affects single pile response and the interaction between piles is explored, and illustrated through an example which shows the relative non-linearity of pile group response by comparison with a single pile, and the average shaft and base responses. An equivalent pier analogue of pile groups and piled rafts is proposed as the most direct method of estimating the stiffness of complete piled foundations, and new design principles are introduced for piled rafts, with the aim of minimising differential settlements by optimal location of the pile support beneath the raft. The various approaches are illustrated through case histories and example applications.

INTRODUCTION

In the majority of cases where piles form part of the foundation for a building or other structure, the primary reason for inclusion of the piles will be to reduce settlements. However, once the decision has been made that piles are required, the traditional design approach has been to ensure that the total structural load can be carried by the piles, with an adequate factor of safety against bearing failure. The nature of load transfer between pile and soil, particularly where shaft friction provides a significant component of the total pile capacity, will then automatically lead to small settlements.

With the above philosophy, design calculations for pile groups concentrate on the ultimate capacity of each pile, treating it in isolation. It is rare that any quantitative allowance is made for differences in capacity between a single isolated pile and one within a group, apart from a check for block failure where the piles are closely spaced. However, the effective stress state in the soil around the pile will generally be significantly different for piles in a group, compared with an isolated pile. Thus, Vesic (1969) has shown that the shaft capacity of piles driven into sand can be greatly enhanced by the installation of neighbouring piles. A similar effect, although probably less marked, is likely for driven piles in lightly overconsolidated clay. In addition, for free-draining soils, the increased effective stress level due to the structural load applied to neighbouring piles will enhance the capacity of each pile within the group. This effect has been remarked upon by Van Weele (1993) in relation to higher pile capacities observed from pile tests conducted using kentledge as reaction rather than, or in addition to, adjacent tension piles.

Design calculations for a pile group, based on summing the capacity of each single pile, will generally prove adequate (if overly conservative), since most group effects are beneficial. However, leaving aside the case of block failure of closely spaced piles, which is a straightforward calculation, situations where the reverse is true include:

poorly constructed continuous flight auger piles in sand, where significant reduction in effective stress levels can occur due to excessive extraction of soil, with the effect likely to be cumulative for large pile groups (Thorburn et al, 1993; Viggiani, 1993);

piles end-bearing on a relatively thin layer of competent soil, overlying weaker material (Goosens and Van Impe, 1991).

The latter case, in particular, is a common trap, and emphasises the importance of considering the overall geometry of the foundation in the design process. As will be discussed later in this paper, engineers should be encouraged to prepare correctly scaled elevation drawings of the complete foundation and relevant soil stratigraphy, which will often reveal shortcomings in the proposed foundation scheme.

While relatively simple analytical methods for estimating the settlement of pile groups have existed for the last two decades, such calculations have tended to be secondary to those for ensuring adequate bearing capacity. The dominance of capacity-based design - which is still evident in current revisions of national and regional design codes - may be attributed in part to the lack of experience many engineers have for estimating the stiffness of soil, and the perception that predicting deformations is less reliable than predicting capacity. In reality, however, the reverse is often true for pile foundations.

Van Impe (1991) has provided an extensive, and somewhat daunting, review of factors that affect the capacity of single piles, from which it is clear that construction techniques, and stress changes that take place in the ground during pile installation, can have a major influence on pile capacity. However, the pile head stiffness (load divided by settlement) at moderate working load levels is rather less sensitive to variations in construction. Thus, consider a situation where the normal effective stress adjacent to a cast-in-situ pile is reduced from the ambient (K_0) value by a factor of 4, due to poor construction. The shaft friction will be lowered correspondingly (although some increase in the amount of dilation as shearing develops will tend to moderate the loss in shaft friction). However, as will be shown later, reduction in soil modulus by a factor of 2 adjacent to the pile (taking modulus proportional to the square root of the effective stress level) will only result in a 20 - 25 % decrease in the local load transfer stiffness. Allowing for integration of the load transfer response along the pile length, the reduction in pile head stiffness will be even less.

There are thus a number of compelling arguments for moving towards a settlement-based design methodology for pile foundations. Of course, in

some cases piles are required purely from a capacity point of view, and the pile group stiffness is of lesser concern (foundations for offshore platforms being an obvious case). However, in most conventional onshore developments, the primary design calculations should reflect the main purpose of the piles, which is to limit settlement. Essentially, piles should be regarded as providing reinforcement for the ground beneath the structure and, in common with other branches of engineering that deal with composite materials, such as reinforced concrete, the focus of analysis should lean towards the global response of the composite, rather than towards the detailed response of each reinforcing fibre.

A variety of numerical and analytical techniques have been developed for calculating the settlement performance of single piles, pile groups and piled rafts, and these are reviewed briefly in the following section. However, it is important to distinguish between the processes of design and analysis. The former process requires relatively simple models, where parametric studies of the effect of pile geometry and soil properties may be undertaken in order to arrive at a viable foundation design with minimal computational effort. More sophisticated analysis is generally reserved for verification and fine-tuning of the design, rather than conception.

Analytical methods, by their nature, require soil parameters as input in order to provide estimates of pile settlement. Since the stress-strain response of soil is non-linear, it is necessary to consider what strain (or stress) is relevant for pile foundations, and how non-linear effects may be incorporated into analyses based on interaction. These aspects of pile group design are considered in later sections of the paper.

The present paper describes both the emerging, settlement-based, philosophy of pile foundation design, and also simple methods which may be used in the design process to quantify performance of the foundation. While many of the ideas may be applied to any type of pile foundation, the paper focuses on situations where the main aim is to limit settlements (particularly differential settlements) with the use of a minimum number of piles. Application of the methods is illustrated through examples with relatively simple geometry (generally pile groups which are square in plan) and soil stratigraphy, since the aim is to establish principles of design rather than demonstrate the full capabilities of modern computational techniques.

In general, it is neither necessary nor economically viable to design pile foundations that reduce settlements to negligible proportions, merely because of a lack of confidence in the ability to predict foundation performance accurately. Since the primary purpose of most piles is to satisfy a serviceability limit on deformations, the design methodology should reflect this, rather than be based on a notional factoring of the ultimate limit state of each pile. Thus, pile groups should be treated as an entity, effectively providing reinforcement of the bearing stratum. The engineer's task is then to optimise cost and performance, using the minimum number of piles, in the most appropriate locations, to provide the required level of reinforcement.

ANALYTICAL TECHNIQUES

Boundary Element Approach

The most rigorous treatment of piles and pile groups is provided by the boundary element method (BEM) as described by Banerjee and Butterfield (1981), Poulos and Davis (1980) and Poulos (1989). In principle, the full interface between soil and foundation units (piles and pile cap or raft) is divided into elements, and an appropriate Green's function (generally that due to Mindlin (1936)) is used to relate the (average) displacement of each element to the traction on each element. Corresponding equations are written for the structural response of the foundation units, using a finite difference or finite element approach. The two sets of equations, together with that for overall equilibrium, allow the

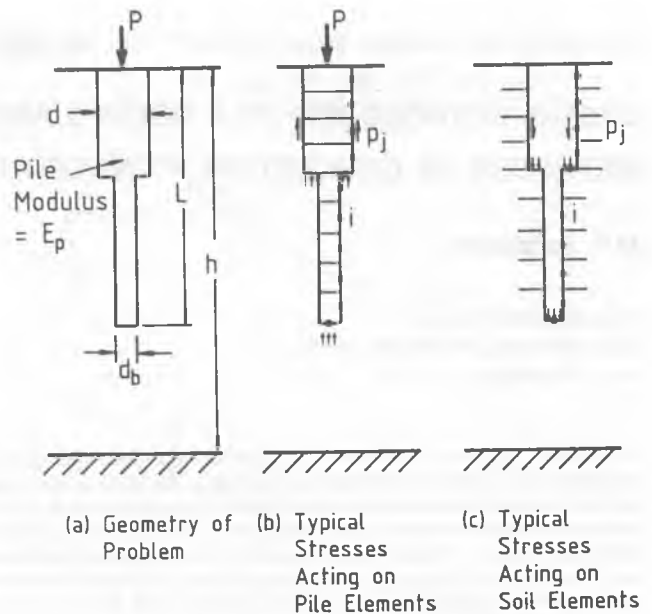


Figure 1 Boundary element analysis of single pile (after Poulos, 1989)

unknown tractions to be found, and hence the stiffness and load distribution throughout the foundation to be evaluated. Figure 1 illustrates the process schematically for a single pile.

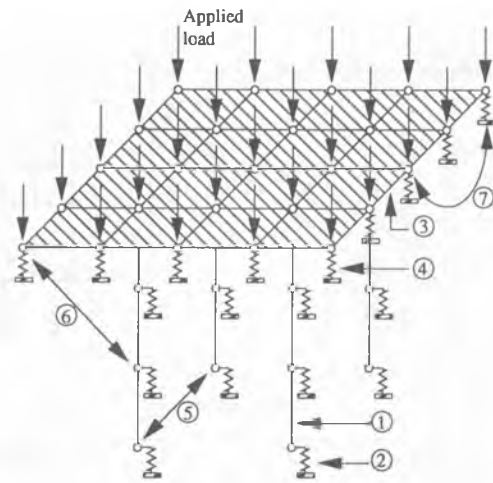
In practice, the computational resources required to perform the ideal analysis described above become excessive for all but the simplest foundation systems. It is therefore necessary to introduce a number of simplifications, perhaps the most effective of which is the combination of a load transfer approach to quantify the relationship between local traction and displacement along each pile, together with the elastic solution of Mindlin to calculate additional displacement due to the tractions acting on the elements of all other foundation units. In that way, non-linear effects may be incorporated explicitly (through the load transfer functions) in the diagonal elements of the flexibility matrix for the pile-soil system. This approach has been used by O'Neill et al (1977), Chow (1986) and Griffiths et al (1991).

For piled rafts, where load is transmitted directly between the pile cap and the ground as well as through the piles, bending deformation of the raft must be taken into account, together with interaction effects through the soil between each raft element and between raft elements and each pile element. Clancy and Randolph (1993) have described an analysis of this type, using a linear load transfer approach for each pile, but otherwise taking full account of interaction between the various foundation elements, as indicated in Figure 2.

Another form of simplification, which reduces significantly the size of the equation set, is the use of interaction factors to represent the influence of a complete foundation unit (for example a pile, or the pile cap) on the displacement of another foundation unit. An interaction factor, α , gives the proportion of the settlement of unit, j , due to its own load acting alone, that is undergone by unit, i (see Figure 3). Algebraically, assuming loads P_i and P_j acting on foundation units which have stiffnesses k_i and k_j , the settlement of unit i is given by

$$w_i = \frac{P_i}{k_i} + \alpha_{ij} \frac{P_j}{k_j} \quad (1)$$

An analysis based on interaction factors proceeds by first evaluating the



1. One-dimensional pile element
2. Ground resistance at each pile node represented by non-linear 'T-Z' springs
3. Two-dimensional plate-bending finite element raft mesh
4. Ground resistance at each raft node represented by an equivalent spring
5. Pile-soil-pile interaction effects calculated between pairs of nodes using Mindlin's equation
6. Pile-soil-raft interaction
7. Raft-soil-raft interaction

Figure 2 Numerical representation of piled raft (after Clancy and Randolph, 1993)

interaction factors between each dissimilar pair of foundation units (principally, each pair of piles of differing spacing and also, for a piled raft, each pile and raft element). This stage of the analysis may be accomplished using either a full boundary element formulation, or the combined load transfer and Mindlin equation approach (Bilotta et al, 1991). Deformation of the raft is then analysed with the piles represented by interacting, and potentially non-linear, springs. Poulos (1993) describes an analysis of this type and further simplifications to facilitate the calculation of interaction between the various foundation units.

As may be deduced from the above discussion, the rigour of the boundary element approach is necessarily diluted by a variety of approximations in order to analyse foundations of practical proportions. Further limitations occur in the application of Mindlin's solution in situations where the soil stiffness is heterogeneous, either vertically due to natural stratification, or horizontally due to the combined effects of pile installation and non-linear stress-strain response of the soil. Poulos (1979) and Yamashita et al (1987) have discussed the choice of appropriately weighted average modulus values when applying Mindlin's equation for heterogeneous soil conditions.

It will be shown later that, for large groups of piles (100 and over), the accuracy of available computer programs is probably no better than $\pm 20\%$ (as indicated by the range of computed results). While such an accuracy is probably sufficient, given the difficulty in estimating the deformation parameters of the soil, it indicates a limit to the extent to which it is fruitful to conduct 'rigorous' analysis of pile groups.

Equivalent Pier or Raft

An alternative approach to detailed treatment of the interaction between each foundation unit, is to consider the foundation as a whole. Traditionally, the settlement of a pile group has been estimated by

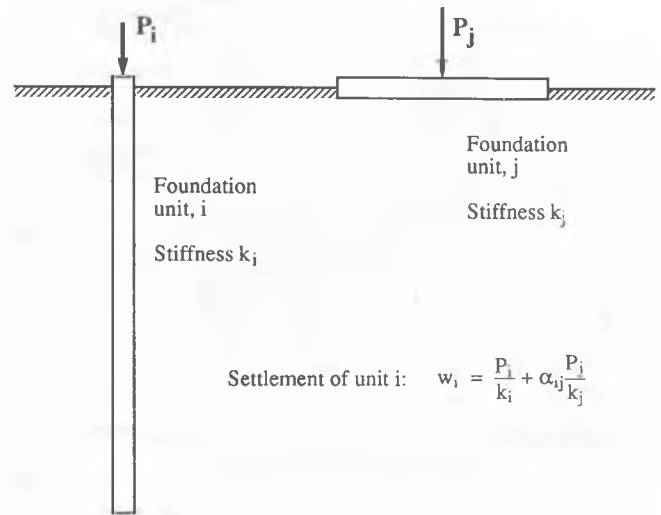


Figure 3 Interaction between two foundation units

considering an 'equivalent' raft, situated two-thirds of the way down the part of the piles which penetrate the main founding stratum, or at the level of the pile bases for end-bearing piles (see Figure 4). The average settlement at ground level is then calculated as

$$w_{avg} = w_{raft} + \Delta w \quad (2)$$

where Δw is the elastic compression of the piles above the level of the equivalent raft, treated as free-standing columns.

Various approaches have been suggested for the area of the equivalent raft, and the method used to calculate the raft settlement, w_{raft} . As indicated in Figure 4, a load-spread of 1 in 4 is generally assumed in order to evaluate the size of the raft.

The main advantage of the equivalent raft approach is that it enables due account to be taken of variations in soil stiffness below the level of the raft. This is of particular relevance in situations where a layer of softer soil exists at some level below the base of the piles. Poulos (1993) has outlined a method of calculation based on elastic influence factors for the vertical strain distribution beneath a raft foundation. The raft settlement is evaluated by integrating the vertical strains, allowing for variations in soil modulus and correcting for the raft embedment below the ground surface using the solutions of Fox (1948).

Algebraically, this approach may be expressed as:

$$w_{raft} = F_D q \sum_{i=1}^n \left(\frac{I_e}{E_s} \right)_i h_i \quad (3)$$

where q is the average pressure applied to the raft, I_e is an influence factor from which the vertical strain may be calculated (see Figure 5), h_i and $(E_s)_i$ are the thickness and Young's modulus respectively for the i^{th} layer, and F_D is the correction factor from Fox (1948). For consistency, the embedment depth should be taken as that below the top of the main bearing stratum, rather than ground surface. The strain influence factors shown in Figure 5 are for the centre-line of a rectangular raft. In order to obtain the average raft settlement, the settlement calculated from equation (3) should be reduced by approximately 20%.

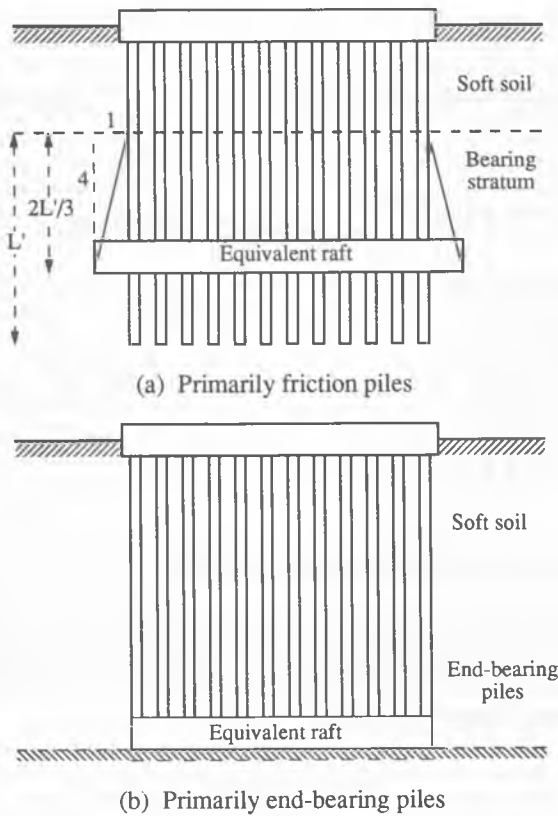


Figure 4 Equivalent raft approach for pile groups

An alternative to the equivalent raft approach, is to consider the region of soil in which the piles are embedded as an equivalent continuum, effectively replacing the pile group by an equivalent pier (Poulos and Davis, 1980). For a pile group of area A_g , the diameter of the equivalent pier may be taken as

$$d_{eq} = \sqrt{\frac{4}{\pi} A_g} = 1.13 \sqrt{A_g} \quad (4)$$

and the Young's modulus of the pier as

$$E_{eq} = E_s + (E_p - E_s) \left(\frac{A_p}{A_g} \right) \quad (5)$$

where E_p is the Young's modulus of the piles, E_s is the (average) Young's modulus of the soil penetrated by the piles and A_p is the total cross-sectional area of the piles in the group. In principle, the equivalent pier should be modelled as a transversely isotropic inclusion, with values of horizontal modulus, E_h , and shear modulus, G_{vh} , close to those for the unreinforced soil.

The load-settlement response of the equivalent pier may be calculated using solutions for the response of a single pile, such as that presented by Randolph and Wroth (1978) (see also Section 4 of this paper) or by charts (see Poulos and Davis (1980)). The overall aspect ratio of the pier will generally be rather low, and solutions for rock-socket response (for example, Carter and Kulhawy (1988)) are particularly suitable. As for the case of the equivalent raft approach, the equivalent pier will furnish an

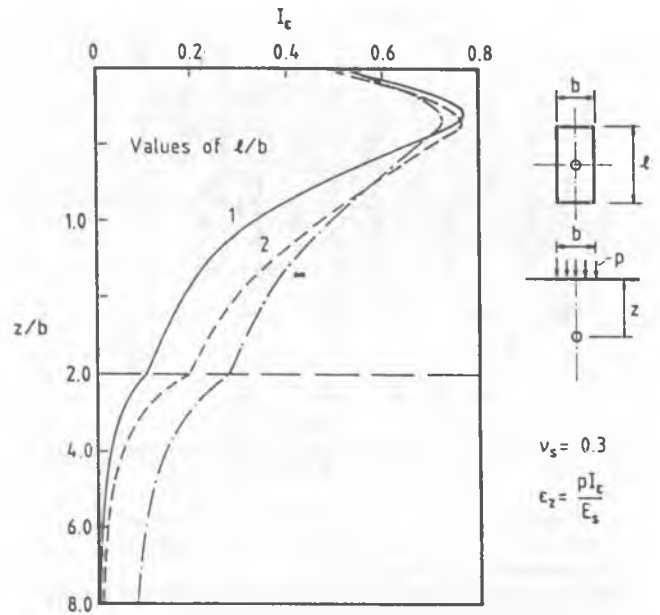


Figure 5 Influence factor for vertical strain (after Poulos, 1993)

estimate of only the average settlement of the pile group, not the differential settlement.

The relative merits of the equivalent raft and pier approaches may be assessed by considering the overall aspect ratio of the pile group, as shown in Figure 6. For a square group of n piles, at spacing, s , and embedded length, ℓ , the overall aspect ratio is $[(\sqrt{n} - 1)s + d]/\ell$ (or approximately \sqrt{ns}/ℓ). However, as will be discussed later in respect of differential settlements of pile groups, it has been found that the degree to which the pile group behaves like a raft foundation also depends on the degree of interaction between the piles, which is categorised by the ratio ℓ/s . As such, an appropriate parameter to categorise pile groups is (Randolph and Clancy, 1993):

$$R = \sqrt{\frac{ns}{\ell}} \quad (6)$$

For values of R which are greater than 4, it will be shown later that the pattern of differential settlement (assuming a fully flexible pile cap) is very similar to that for a raft foundation. An equivalent raft would therefore be a logical analogue for analysis. For smaller values of R , and certainly for values less than 2, it would seem at the outset that an equivalent pier approach is more logical, at least for estimating average settlements.

SOIL PROPERTIES

Although there are a number of situations where piles will mobilise limiting shaft friction over part of their length under working conditions, the performance of most pile groups may be assessed in terms of elastic parameters for the soil. However, it is necessary to consider effects of non-linearity prior to failure when assessing interaction effects (Jardine et al, 1986).

To a first approximation, the deformation mode of the soil around a vertically loaded pile resembles the shearing of concentric cylinders (Frank, 1974). As such, the relevant elastic parameter is the shear modulus, G . Conventionally, the value of shear modulus is assumed to be

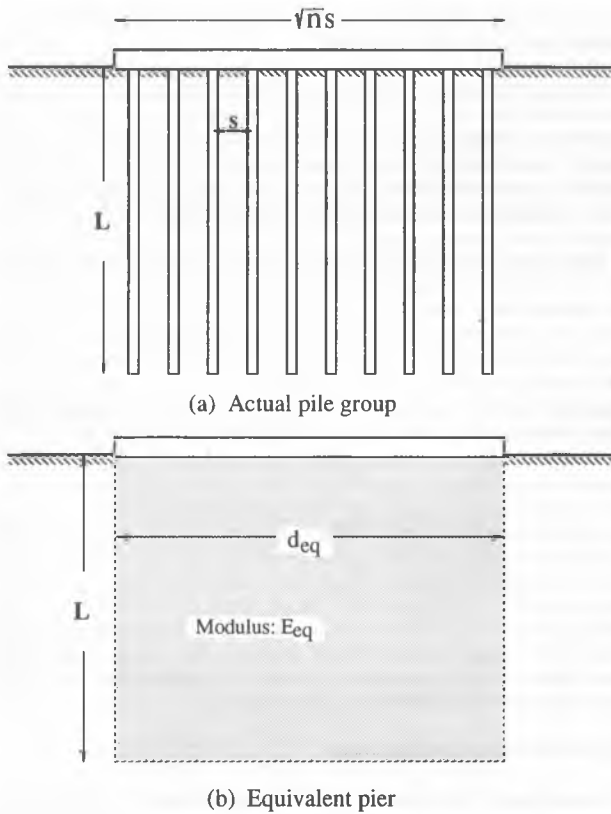


Figure 6 Replacement of pile group, or piled raft, by equivalent pier

independent of whether the soil deformation is drained or undrained, which is a further reason to base solutions on shear modulus rather than Young's modulus, E , although the two parameters may be related via Poisson's ratio, ν , as $E = 2G(1 + \nu)$.

Low-Strain Shear Modulus

Major advances have occurred in the past decade in establishing the variation of secant modulus with shear stress or shear strain level. The current understanding points to the existence of a limiting shear modulus, G_0 , at small strain (less than about 0.001 %), with the secant modulus reducing by an order of magnitude at the point of failure. It is therefore essential to consider the shear strain and shear stress levels in the soil in the vicinity of pile foundations, in order to estimate the deformation under working conditions.

The first step is to consider the relationship between shear strain and deformation of a single pile. For a linear elastic soil response, assuming a shearing mode of concentric cylinders around the pile, Randolph and Wroth (1978) showed that the local load transfer response at the pile shaft may be written:

$$w_s = \zeta \frac{\tau_0 r_0}{G} \quad (7)$$

where w_s is the pile displacement, τ_0 is the shear stress, and r_0 is the pile radius. The parameter, ζ may be thought of as a geometry factor, relating the normalised displacement, w_s/r_0 to the shear strain, $\gamma_0 = \tau_0/G$, adjacent to the pile. The value of ζ is given by

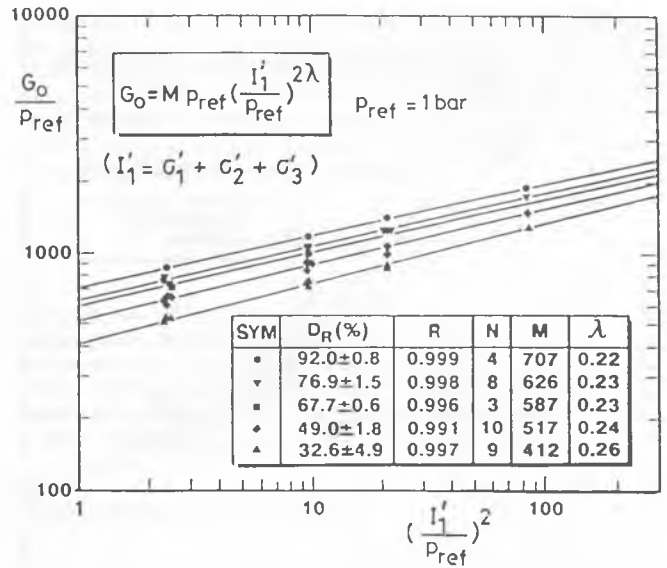


Figure 7 Small strain shear modulus of Hokksund sand (Carriglio, 1989)

$$\zeta = \ell n(r_m / r_0) \quad (8)$$

where r_m is the maximum radius of influence of the pile, which in turn is related to the pile length by (Randolph and Wroth, 1978)

$$r_m \approx 2.5\rho(1 - \nu)\ell \quad (9)$$

where ρ is a parameter which reflects the vertical homogeneity of the soil stiffness, varying from unity for homogeneous conditions, to 0.5 where the stiffness is proportional to depth.

For typical pile slenderness ratios, ℓ/r_0 , the value of ζ will lie in the range 3.5 to 4.5, and it is often sufficiently accurate to adopt a value of 4. Equation (7) may then be used to assess the strain level in the soil. Thus, it is generally accepted that full mobilisation of shaft friction occurs at a relative pile-soil displacement of about 1 % of the pile diameter (2 % of the radius). Assuming a linear soil response, this implies local shear strains in the soil adjacent to the pile shaft of about 0.0125 %. Since the shear stress (and shear strain, for linear soil response) varies approximately inversely with distance from the pile axis, at the closest common pile spacing of three diameters (six pile radii), the strain level at the position of a neighbouring pile would be $0.0125/6 = 0.002$ %.

In practice, non-linearity of soil response will lead to higher shear strain levels adjacent to the pile, although shear strains in the vicinity of neighbouring piles will tend to be lower. Under working conditions, the mobilised shear stress adjacent to the pile will rarely exceed 50 % of the shear strength of the surrounding soil. At a typical minimum pile spacing of three diameters, the mobilised shear stress will thus be less than 10 %. This confirms that the appropriate value of shear modulus for estimating interaction effects is the 'low-strain' or initial shear modulus, G_0 . The low-strain shear modulus appears to be a very reproducible quantity, that correlates closely with the square root of the mean effective stress for sands.

Figure 7 shows correlations of initial shear modulus presented by Van Impe (1991) (based on results of Carriglio (1989), original reference not cited) for Hokksund silica sands, which are consistent with a relationship of the form

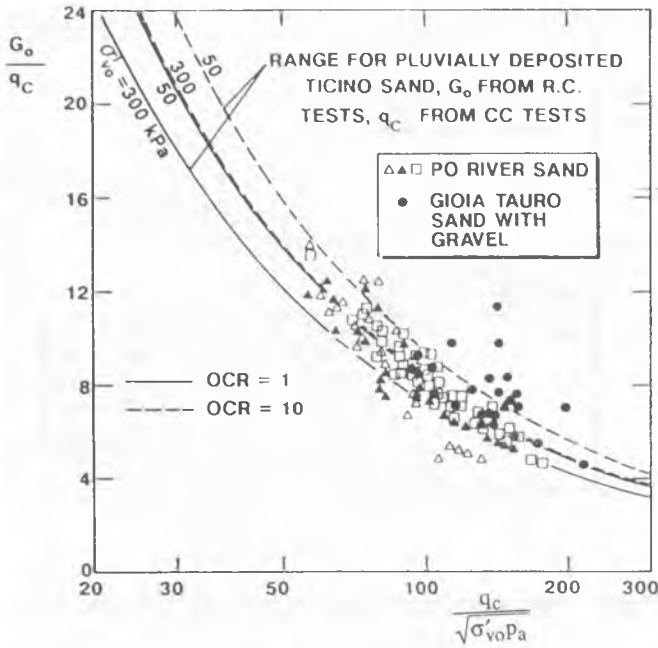


Figure 8 Correlation of G_0 , q_c and σ'_{v0} (after Baldi et al, 1989)

$$\frac{G_0}{p_a} = 400(1 + 2I_D) \left(\frac{p'}{p_a} \right)^{0.5} \quad (10)$$

where I_D is the relative density, p' is the mean effective stress and p_a is atmospheric pressure (100 kPa). The value of the modulus number (400) and the exponent (0.5) will vary for different soils. The exponent will generally lie in the range 0.4 to 0.55, while the modulus number decreases with increasing silt content of the soil.

Alternatively, the initial shear modulus may be correlated with the results of in situ tests such as the cone resistance, q_c , or, as a last resort, the SPT blow-count, N . The ratio G/q_c may be taken as a function of the relative density of the soil, which is in turn reflected by the ratio of cone resistance to the in situ effective vertical stress, σ'_{v0} . It has been common to correlate G/q_c with the quantity $q_c/\sqrt{p_a\sigma'_{v0}}$ (Robertson, 1991) as shown in Figure 8. This correlation is broadly consistent with recommendations by Imai and Tonouchi (1982), of

$$\frac{G_0}{p_a} \approx 50 \left(\frac{q_c}{p_a} \right)^{0.6} \quad (11)$$

Although a linear correlation of soil modulus with SPT count is often adopted for convenience, a sub-linear correlation appears to fit the data better. Wroth et al (1979) have discussed a range of correlations, based on the work of Ohsaki and Iwasaki (1973) and other workers, that may be written as:

$$\frac{G_0}{p_a} \approx 120N^{0.8} \quad (12)$$

The above correlations of initial shear modulus with cone resistance and SPT count may also be applied to clay soils. However, it is often more

convenient to correlate shear modulus directly with either undrained shear strength, s_u , or mean effective stress, p' .

Jardine et al (1986) report ratios of small strain modulus to shear strength which range from $G_0/s_u = 500$ to 1000. This range is consistent with data presented by Kagawa (1992), who found that the initial shear modulus was directly proportional to consolidation stress (for normally consolidated samples), with a typical ratio of $G_0/\sigma'_c = 160$. Assuming a strength ratio of $s_u/\sigma'_c = 0.25$, the implied rigidity index is $G_0/s_u = 640$.

A direct correlation of shear modulus with shear strength oversimplifies the true picture, where the rigidity index will also vary with overconsolidation ratio (OCR). In addition, some experimenters have found the initial shear modulus varies with effective stress level to some power less than unity. The effective stress exponent varies from as low as 0.5 (Hardin and Black, 1968; Lo Presti et al, 1991) to unity, with a tendency for the exponent to increase with increasing plasticity index. Thus Viggiani (1991) has expressed the initial shear modulus as

$$\frac{G_0}{p_a} = A(OCR)^m \left(\frac{p'}{p_a} \right)^n \quad (13)$$

with typical values of m close to 0.25. For four different clays, she quotes values of n varying from 0.65 (kaolin, low plasticity) to 0.85 (Fucino clay, high plasticity), with corresponding values of the modulus number, A , that range from 500 (kaolin) down to 200 (Fucino clay).

Hyperbolic Stress-Strain Response

The adoption of low-strain, or initial, values of shear modulus such as those implied by the foregoing correlations must be accompanied by correct treatment of the non-linear soil response in order to assess the settlement of each individual pile. A convenient model is provided by the hyperbolic approximation, where the secant shear modulus, G , varies linearly with the shear stress level according to

$$\frac{G}{G_0} = 1 - R_f \frac{\tau}{\tau_f} \quad (14)$$

where τ_f is the failure shear stress and R_f is a parameter that dictates the degree of curvature of the stress-strain response. Values of R_f are generally taken in the range 0.9 - 1. In practice, real soils often show a more rapid decrease of secant modulus with shear stress level, which may be described better by a relationship of the form (Fahey and Carter, 1993)

$$\frac{G}{G_0} = 1 - f \left(\frac{\tau}{\tau_f} \right)^g \quad (15)$$

where the parameter, f , plays a similar role to R_f in equation (14), dictating the ratio G/G_0 at failure.

Most natural soils, particularly those of significant age, show a very rapid drop in shear stiffness once the threshold shear strain is reached, and values of the parameter g as low as 0.25 may appear appropriate (Fahey and Carter, 1993). The rapid reduction in stiffness is linked with high values of initial shear modulus, in excess of those correlations suggested previously. By contrast, soil samples prepared in the laboratory, or those that have suffered minor disturbance due to sampling, will show a lower initial shear modulus, and a more gradual reduction in secant shear modulus that may be matched with g values in the range 0.7 - 1.

Around the pile shaft, the shear stress decreases inversely with the radius,

and a significant proportion of the pile displacement is contributed by soil at relatively low shear stress levels. As such, the resulting load transfer curve is much less non-linear than the original stress-strain curve of the soil. This feature is discussed in more detail in the following section.

At the base of the pile, the deviator stress decays essentially with the square of the distance from the pile tip, and the displacement field is more localised. The resulting load-displacement response of the pile base is adequately represented directly by a hyperbolic curve (Fleming, 1992). At typical working load levels for pile groups, the secant shear modulus for the base response will be about 50 % of the initial, low-strain, value.

SINGLE PILE RESPONSE

Elastic solutions for the axial response of a single pile have been presented by a number of authors, starting with the boundary element solutions of Poulos and Davis (1968), Poulos (1968) and Butterfield and Banerjee (1971). Randolph and Wroth (1978) presented an approximate solution, based on separate treatment of the pile shaft, using the linear load transfer function of equation (7), and the pile base, using the Boussinesq solution for a rigid punch acting on an elastic half-space. The solution allows for a linear increase of shear modulus with depth, with an average value of ρG_ℓ where G_ℓ is the value in the vicinity of the pile base. The pile head response is given by

$$\frac{P_t}{G_\ell r_o w_t} = \frac{4\eta}{(1-\nu)\xi} + \rho \frac{2\pi \tanh \mu \ell}{\zeta} \frac{\mu \ell}{\mu \ell} \frac{\ell}{r_o} \quad (16)$$

where P_t and w_t are the load and displacement at the top of the pile, ℓ and r_o are the length and radius of the pile, G_ℓ is the value of shear modulus at a depth of $z = \ell$. The other parameters are given below, where the subscript b refers to conditions at or below the pile base:

$$\begin{aligned} \eta &= r_b/r_o && \text{(under-reamed piles)} \\ \xi &= G_\ell/G_b && \text{(end-bearing piles)} \\ \rho &= G_{avg}/G_\ell && \text{(heterogeneity of soil modulus)} \\ \lambda &= E_p/G_\ell && \text{(pile-soil stiffness ratio)} \\ \zeta &= \ell n(r_m/r_o) \\ r_m &= \{0.25 + \xi[2.5\rho(1-\nu) - 0.25]\} \ell && \text{(maximum radius of influence)} \\ &= 2.5\rho(1-\nu)\ell \text{ for } \xi = 1 \text{ (friction pile)} \end{aligned}$$

$$\text{and } \mu \ell = \sqrt{2/\zeta \lambda} (\ell/r_o) \quad \text{(pile compressibility).}$$

The proportion of load reaching the pile base is given by

$$\frac{P_b}{P_t} = \frac{4\eta}{(1-\nu)\xi} \frac{1}{\cosh \mu \ell} \quad (17)$$

For long piles, or where the stiffness ratio is low (as in a rock-socketed pile), very little load will reach the base of the pile, and the pile response becomes independent of the pile length. Thus, for piles longer than $\ell/r_o = 3\sqrt{E_p/G_\ell}$, the pile head stiffness may be approximated as

$$\frac{P_t}{G_\ell r_o w_t} \approx \rho \pi \sqrt{2\lambda/\zeta} \quad (18)$$

with G_ℓ taken as the shear modulus at a depth of $z = 3r_o\sqrt{E_p/G_\ell}$.

Although originally intended for piles of slenderness ratio, ℓ/d , in excess of about 10, the above solution remains surprisingly accurate for even shorter piles. Carter and Kulhawy (1988) have compared the solution with more rigorous numerical analyses of stubby rock-socketed piles, and show errors of only 20 - 30 % even for values of ℓ/d as low as 2. In fact, the solution may be rendered more accurate for very stubby piles by adjusting the expression for the parameter, ζ , according to

$$\zeta = \ell n[5 + 2.5\rho(1-\nu)\ell/r_o] \quad (19)$$

The addition of the constant term makes insignificant difference for normal piles (with ℓ/d of 10 or more) but increases the pile head flexibility for shorter piles in keeping with the accurate solutions of Poulos and Davis (1980) and Carter and Kulhawy (1988). The adjusted solution may be applied to the analysis of equivalent piers (see Section 5) and thus provides a simple approach for estimating the stiffness of pile groups.

Solution for Non-Linear Soil Response

It has been customary to model the complete load-displacement response of a pile by means of a hyperbolic function, particularly in order to extrapolate the results of load tests to yield estimates of ultimate failure load (Chin, 1970; 1972). The hyperbolic representation does not always give an acceptable fit to the measured response, and a considerable improvement has been developed by Fleming (1992), whereby the shaft and base response of the pile are modelled by separate hyperbolic functions, and then combined making due allowance for elastic shortening of the pile. This approach enables a very close fit to measured test results to be obtained, and offers the potential for use as a predictive approach.

Modelling the pile base response by a hyperbolic function appears an acceptable approach, at least for cast-in-situ piles, since the soil displacement field is relatively localised beneath the pile tip, and large displacements (by comparison with the initial elastic response) are required to develop the ultimate load. However, some caution is necessary before applying a similar technique to the shaft response, where a significant proportion of the shaft displacement occurs far from the pile, in soil at relatively low shear stress levels, and the ultimate condition is reached rather abruptly, at displacements of the order of 1 % of the pile diameter.

The shape of the load transfer response along the pile shaft may be deduced for any given stress-strain response of the soil, by integrating the shear strains around the pile, in the manner that led to the linear load transfer relationship of equation (7). Integration is carried out between the pile radius, r_o and the maximum radius of influence, r_m , maintaining the assumption of shear stress varying inversely with radius. For a hyperbolic stress-strain response, where the shear modulus is given by equation (13), the load transfer parameter, ζ , becomes

$$\zeta = \ell n \left[\frac{r_m/r_o - \psi}{1 - \psi} \right] \quad (20)$$

where $\psi = R_f \tau_o/\tau_s$, where τ_o is the shear stress at the pile shaft and τ_s is the limiting shaft friction (for example, Kraft et al, 1981).

Figure 9 shows non-linear load transfer curves obtained from a hyperbolic stress-strain response, for R_f values of 0.95 and 1. The initial value of ζ (for $\psi = 0$) has been taken as 4, and the ratio G_o/τ_s as 400. For comparison, a parabolic curve is also shown, of the form

$$\frac{w}{r_o} = m \zeta \frac{\tau_s}{G_o} \left[1 - \left(1 - \frac{\tau_o}{\tau_s} \right)^{1/m} \right] \quad (21)$$

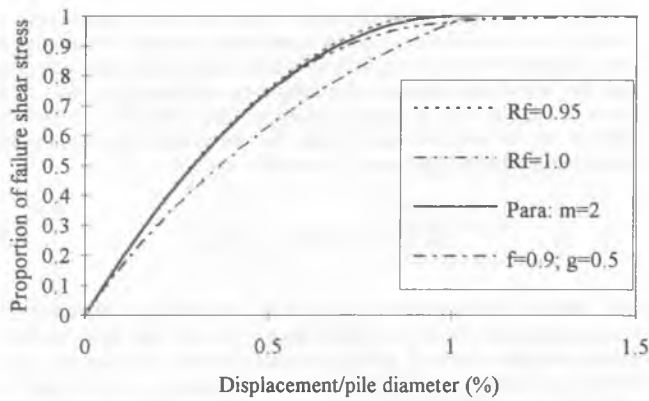


Figure 9 Non-linear load transfer curves based on hyperbolic stress-strain response of soil

with $m = 2$ (keeping ζ constant at 4). It may be seen that this curve provides a good representation of those curves derived from the hyperbolic stress-strain law.

As discussed previously, the measured stress-strain response of many soils is more non-linear than the hyperbolic relationship implies, and the modified form of equation (15) often provides a closer fit. An example load transfer curve using this relationship, taking $f = 0.9$ and $g = 0.5$ is shown in Figure 9. This load transfer curve may be approximated using a hyperbolic relationship directly (equation (14)), taking $R_f = 0.5$.

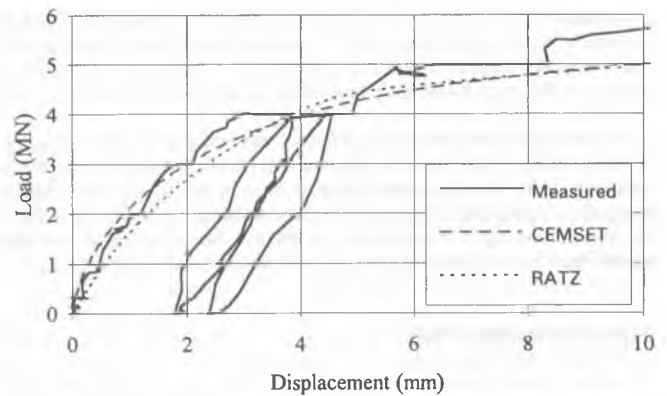
In summary, the original stress-strain response of soil may be fitted using hyperbolic relationships in the form of equations (13) and (14), with R_f (or f) values in the region of 0.9. However, allowance for the variation of shear stress around the pile shaft leads to load transfer curves that are more linear, and correspond to hyperbolic shapes with values of R_f in the region of 0.5 or lower (Poulos, 1989). For most soil types, however, the parabolic representation of equation (21), with m in the range 2 - 3, gives a closer fit to experimental load transfer curves (for example, Aldridge and Schnaid, 1992), than does the use of a hyperbolic curve with a low value of R_f .

An attractive feature of the parabolic shape of load-transfer curve is that full shaft friction is mobilised at a displacement of m times the extrapolated elastic response. Thus, the quantity $(1/m)$ gives the secant gradient at failure as a proportion of the initial tangent gradient, in a similar manner to the quantities $(1 - R_f)$ and $(1 - f)$ for the hyperbolic curves.

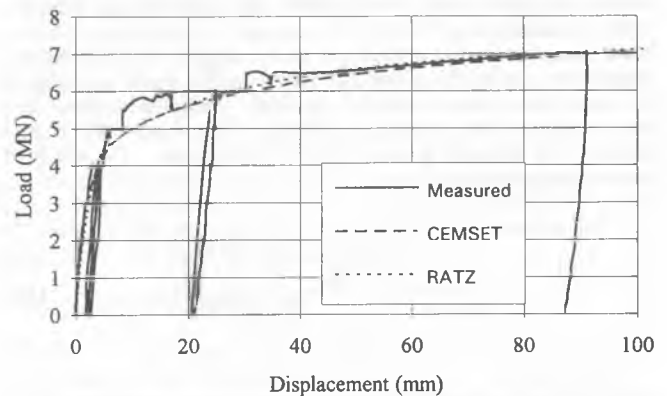
It is of interest to explore differences in deduced design parameters that may arise through adopting (a) direct hyperbolic representations of the pile shaft and base responses, as in the CEMSET approach (Fleming, 1992) or (b) integrated hyperbolic response of the pile shaft (equation (20)) together with an hyperbolic base response, as in the RATZ approach of Randolph (1986).

Figure 10 shows a fit to the measured results of a load test on a bored pile, cast under bentonite, 800 mm diameter by 20 m long. The pile was founded in relatively dense interbedded clayey sands and silts. The pile response at small displacements is shown in the upper diagram for clarity. The fitted responses using CEMSET and RATZ could perhaps be improved on by further adjustment of parameters, but the overall pile response is captured relatively closely.

For both analyses, the Young's modulus of the pile has been taken as 30 GPa regardless of the load level, although, in practice, some non-linearity in the structural response of cast-in-situ piles may be expected. For the CEMSET analysis, ultimate shaft and base loads of 5 MN and 3.1 MN have been deduced, together with a value of the CEMSET non-dimensional shaft flexibility parameter, M_s , of 0.0007, and a base modulus



(a) Small displacements



(b) Overall response

Figure 10 Back-analysis of load test on an 800 mm diameter bored pile

of $E_b = 50$ MPa (nominally at 25 % of the base capacity). The RATZ fit has been obtained with average shaft friction of 85 kPa (shaft capacity of 4.3 MN) and limiting end-bearing pressure of 7 MPa (base capacity of 3.5 MN). Average low-strain shear modulus down the pile shaft was taken as 200 MPa, while the initial base shear modulus was 68 MPa.

The deduced modulus values may be compared, noting that the parameter M_s is equivalent to $0.5\zeta\tau_s/G_0$ where τ_s is the limiting shaft friction. Taking $\zeta = 4$, the CEMSET analysis thus corresponds to an average low-strain shear modulus of $G_0 = 284$ MPa. Similarly, the E_b (at 25 % ultimate) of 50 MPa corresponds to an initial tangent shear modulus of 25 MPa (taking Poisson's ratio equal to 0.3). Table 1 summarises the various parameters.

It may be seen that, while there is agreement to within 4 % on the overall capacity of the pile, other parameters deduced from the back-analyses

Table 1 Parameters deduced from back-analysis of load test

| Parameter | CEMSET | RATZ |
|--|--------|------|
| Ultimate shaft capacity, Q_s (MN) | 5.0 | 4.3 |
| Average shaft friction, τ_s (kPa) | 100 | 85 |
| Avg initial shear mod. (shaft), G_{0s} (MPa) | 284 | 200 |
| Rigidity index, G_{0s}/τ_s | 2840 | 2350 |
| Ultimate base capacity, Q_b (MN) | 3.1 | 3.5 |
| Unit end-bearing pressure, q_b (MPa) | 6.2 | 7.0 |
| Initial shear modulus (base), G_{0b} (MPa) | 25 | 68 |
| Rigidity index, G_{0b}/q_b | 4.0 | 9.7 |
| Ultimate total capacity, Q_t (MN) | 8.1 | 7.8 |

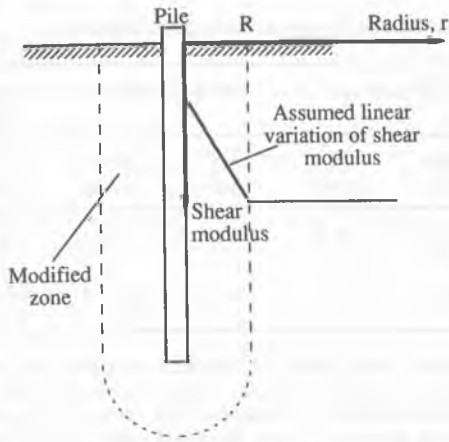


Figure 11 Zone of modified soil around pile due to construction

show a wider variation. In particular, the hyperbolic representation of the shaft response leads to comparatively high estimates of the average shaft friction and tangent shear modulus, and compensating low estimates of the base parameters. Overall, though, it should be emphasised that, however close a fit to the measured data is obtained, the deduced parameters may not necessarily represent reality. Either of the above models (CEMSET and RATZ), or any one of a number of other models, may be used to interpolate the results of a set of load tests in order to predict working pile performance, for the given set of soil conditions and construction method. However, each analytical model has its own short-comings, and the accuracy of any extrapolation to new conditions cannot be guaranteed.

Effects of Pile Construction

As discussed by Van Impe (1991), the method of construction can have an important influence on the capacity and, to a lesser extent, the initial displacement response of a pile. Conceptually, the effect of construction may be modelled by adjusting the soil modulus in a zone around the pile. Poulos (1988) has used this approach to explore construction effects on the interaction between piles, adopting a linear variation of soil stiffness around the pile, as indicated in Figure 11.

For driven piles, the soil stiffness may be expected to be higher in the zone immediately around the pile, while for cast-in-situ piles, the soil stiffness will be reduced. The magnitude of the change in load transfer stiffness may be quantified for any given radial variation of soil stiffness, in the same manner as for a non-linear soil response. Essentially, the load transfer flexibility may be quantified in terms of a modified value of the parameter ζ in equation (7). For a linear variation of shear modulus in the region $r_0 < r < R$, from a value of G_{r_0} adjacent to the pile, the modified value of ζ is given by

$$\zeta^* = \zeta + \ell n \left[\left(R^* G^* \right)^a / R^* \right] \quad (22)$$

where $a = (R^* - 1)/(R^* G^* - 1)$, $R^* = R/r_0$ and $G^* = G_{r_0}/G_0$.

Figure 12 shows the effect on the load transfer flexibility, expressed as ζ^*/ζ , for a range of values of G^* and R^* , taking $\zeta = 4$. It may be seen that, except for extreme changes in soil stiffness adjacent to the pile or very extensive regions of modified soil stiffness, the effect on the load transfer gradient is less than 50%. Since changes in the effective stress regime due to pile construction are difficult to quantify, the effects on pile response may generally be lumped in with those due to non-linear soil response.

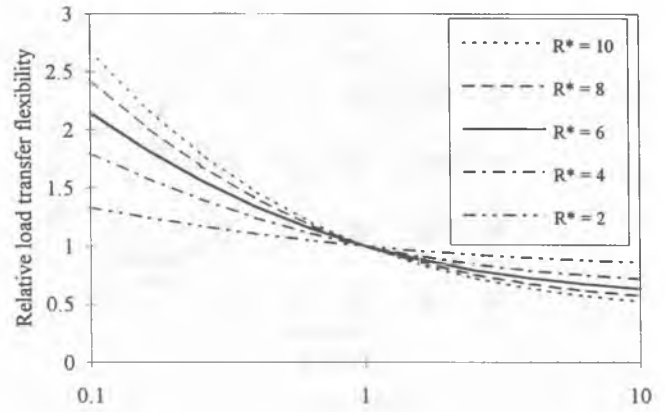


Figure 12 Effect of modified soil zone on load transfer gradient

PILE GROUP RESPONSE

The basis for calculating the response of a pile group, by comparison with that of a single pile, is the principle of elastic interaction between piles. For simplicity, the performance of a pile within a group has generally been expressed in terms of a group settlement ratio (Poulos and Davis, 1980) or efficiency (Fleming et al, 1992), modifying the stiffness of a single pile to account for interaction effects. This approach has some limitations when the soil response is non-linear, since a portion of the (non-linear) settlement of a single pile is localised around the pile, and does not contribute to interaction with neighbouring piles.

However, before considering non-linear effects, a simple approach will be outlined for estimating pile group response, extending the model for a single pile, where the shaft and base responses were considered separately, to an equivalent group pile where the two components are modified according to the degree of interaction.

The solution for a single pile (equation (16)) was based on the assumption of a logarithmic displacement field around the pile shaft. This implies that, if the shaft displacement of a given pile is w_s , then a neighbouring pile at spacing, s , will be subjected to a displacement of $w_s \ell n(r_m/s)/\zeta$ where r_m is the maximum radius of influence of original pile and $\zeta = \ell n(r_m/r_0)$.

The displacement field around the pile tip, treated as a rigid punch, decays essentially inversely with radius. For a base displacement w_b of one pile, the interactive displacement of a neighbouring pile at spacing, s , will be $2w_b r_b / (\pi s)$, where r_b is the pile base radius (Randolph and Wroth, 1979).

The above considerations allow the response of an average pile in a group to be deduced, modifying the shaft and base stiffnesses for a single pile in accordance with the total interaction effect. For a group of n piles, the load transfer parameter, ζ should be replaced by

$$\zeta^* = n\zeta - \sum_{i=2}^n \ell n(s_i / r_0) \quad (23)$$

Similarly, the base stiffness is adjusted by replacing the parameter, ξ , by

$$\xi^* = \xi \left[1 + \frac{2}{\pi} \sum_{i=2}^n \frac{r_b}{s_i} \right] \quad (24)$$

where s_i is the spacing of the i th pile from pile 1.

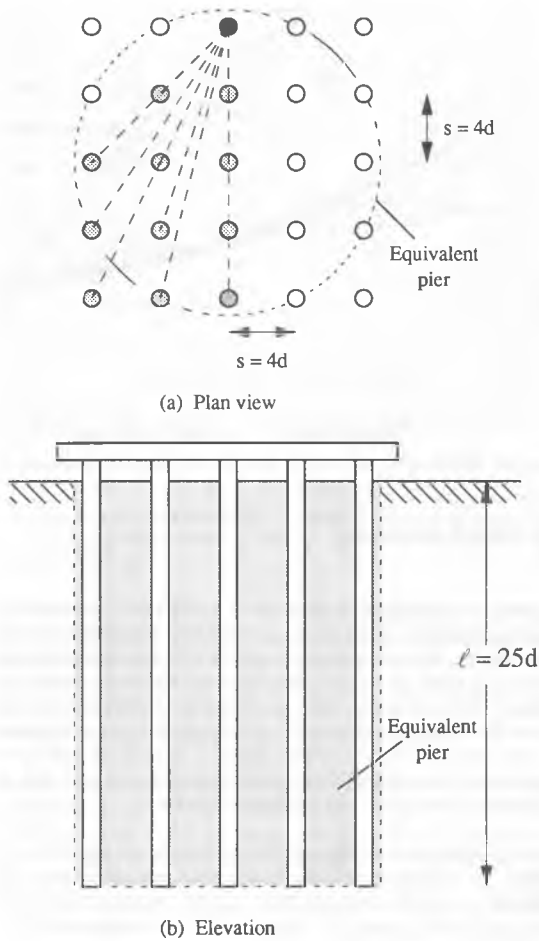


Figure 13 Example 5 x 5 pile group

Equations (23) and (24) may then be used in equation (16) to calculate the response of the typical 'group' pile. Since interaction is greater for the shaft response than for the base response, the net effect is that a greater proportion of the load is transferred to the base of piles in a group than compared with a single isolated pile. For groups of up to 100 piles, the typical pile may be taken as the mid-edge pile, while for larger groups it may be shown that the middle pile in the row adjacent to the edge is more representative.

Figure 13 shows the range of pile spacings that need to be considered in estimating the response of a 5 x 5 pile group. For a pile spacing of $s/d = 4$, pile slenderness ratio of $l/d = 25$, and stiffness ratio of $E_p/G = 1000$, the modified values of ζ and ξ are 43.2 and 2.78 respectively, compared with values of 4.47 and 1 for the single pile. Table 2 shows the resulting group pile stiffness (in terms of the load per pile), which reduces from 54.2 for a single pile to 8.8 for the pile group - an estimated 'efficiency' of $8.8/54.2 = 0.16$. The proportion of load taken by the pile base is estimated to increase from 6.1 % for a single pile, to 21.5 % for the pile group.

For comparison, values of pile head stiffness and load sharing calculated using the numerical approach of Clancy and Randolph (1993) are also shown in Table 2. It may be seen that the approximate method gives a higher pile group stiffness, by about 13 %, compared with the numerical analysis, and indicates a significantly higher proportion of load reaching the pile bases. The difference in the estimated stiffnesses is partly due to the tendency for the numerical analysis to underestimate stiffness by comparison with a full boundary element analysis of the group (for example, Butterfield and Douglas, 1981).

Table 2 Comparison of single pile and pile group response

| | Equations (16) & (17) | | Numerical analysis | | Equivalent pier |
|----------------------------|-----------------------|-------------|--------------------|-------------|-----------------|
| | Single pile | 5 x 5 group | Single pile | 5 x 5 group | 5 x 5 group |
| $\frac{P_t}{G_r \omega_t}$ | 54.2 | 8.8 | 54.3 | 7.8 | 8.9 |
| $\frac{P_b}{P_t}$ | 6.1 % | 21.5 % | 6.1 % | 13.5 % | (41.8 %) |

The final column in Table 2 shows the results of treating the pile group as an equivalent pier. This leads to the highest estimate of pile group stiffness, but is the simplest calculation of the three. The estimated proportion of load reaching the base of the equivalent pier includes all load transmitted between the actual piles, and thus is considerably higher than the values obtained from the other analyses. Interestingly, if an equivalent raft approach were to be used, situated at a depth of $2/3$ the length of the piles and using a 1:4 load spread, the average pressure on the raft would be 43 % of the actual applied pressure, which is comfortably close to the figure from the equivalent pier analysis. The estimated non-dimensional stiffness using an equivalent raft approach is 7.1, which is some 10 - 20 % lower than the other values.

Group Efficiency

Due to interaction effects, the stiffness of each pile in a group is reduced by comparison with a single pile. This may be quantified through the use of an efficiency, η , the inverse of the group settlement ratio, R_s , defined as (Fleming et al, 1992):

$$\eta = \frac{1}{R_s} = \frac{k_p}{nk_1} \quad (25)$$

where k_1 is the pile-head stiffness of a single pile, and k_p is the stiffness of the complete group (in terms of average settlement). To a first approximation, the group efficiency may be taken as a simple power law of the number of piles in the group, as

$$\eta = n^{-e} \quad (26)$$

giving the group stiffness as

$$k_p = n^{1-e} k_1 \quad (27)$$

The exponent, e , generally lies in the range 0.3 - 0.5 for primarily friction piles, rising to 0.6 or higher for end-bearing piles. For friction piles, Fleming et al (1992) present a set of design charts, reproduced in Figure 14, whereby the exponent is expressed in terms of a base value, e_1 , depending on the slenderness ratio of the pile, and four correction factors, c_1 to c_4 , as indicated below:

$$e = e_1(\ell/d) \cdot c_1(E_p/G) \cdot c_2(s/d) \cdot c_3(p) \cdot c_4(v) \quad (28)$$

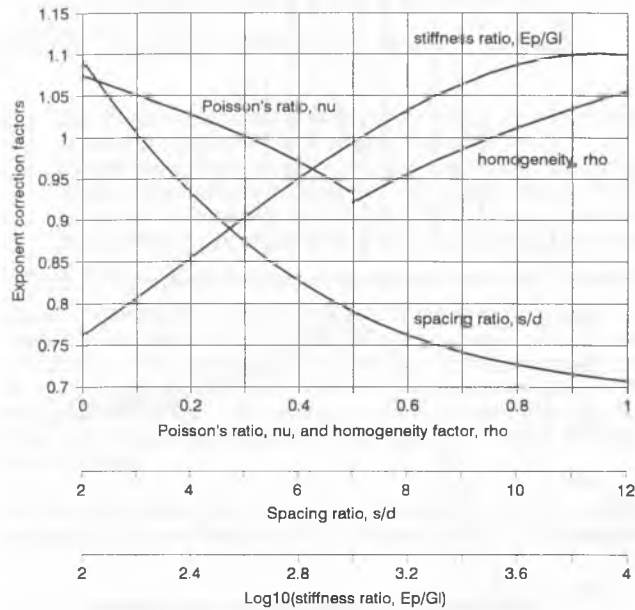
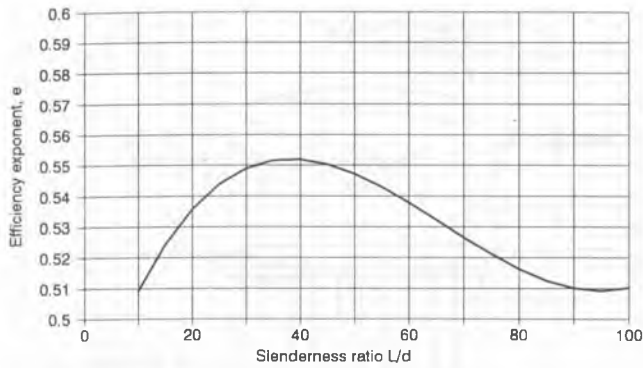


Figure 14 Design charts for group efficiency (after Fleming et al, 1992)

The value of e_1 is based on typical values for pile geometry and soil properties of $E_p/G_\ell = 1000$, $s/d = 3$, $\rho = 0.75$ and $\nu = 0.3$. For the example shown in Figure 13, the values of the various factors are $e_1 = 0.55$, $c_1 = 1$, $c_2 = 0.93$, $c_3 = 1.06$, $c_4 = 1$, giving an overall value of $e = 0.54$. The calculated group efficiency is therefore $\eta = 25^{-0.54} = 0.175$, which is comparable with the approximate method outlined earlier. It may be noticed that typical values of e in the range 0.4 - 0.5 imply group efficiencies which are less than 0.1 for pile groups in excess of 100 piles.

The simple use of efficiency factors, or group settlement ratios, does not provide any indication of the increased proportion of load carried by the pile bases in a group of piles - and thus the greater influence of underlying soil strata compared with the case of a single pile. In addition, as pointed out by Poulos (1993), since the base response is generally more non-linear than the shaft response, this may lead to lower group efficiencies (and thus lower group stiffness) than estimated using linear elasticity. On the other hand, ignoring non-linear effects will overestimate the degree of interaction between piles, which will compensate for overestimation of the base stiffness.

Effect of Soil Non-Linearity on Interaction

It has already been noted that the curvature of the load transfer curve used to describe the pile shaft response is much less marked than that of the

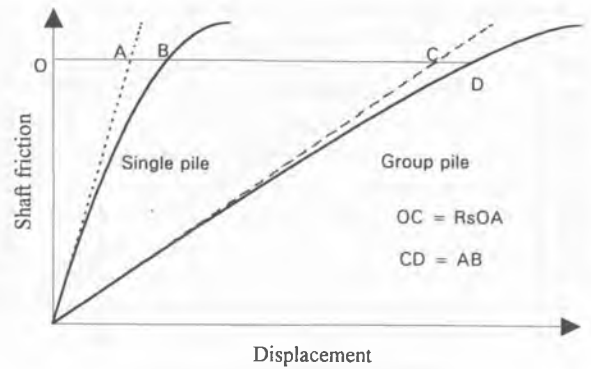


Figure 15 Calculation of interaction with non-linear load transfer curves

original stress-strain response of the soil. However, effects of non-linearity are important when considering interaction between piles, as has been remarked upon by Jardine et al (1986). Radial heterogeneity of soil stiffness, whether due to installation effects that lead to a softened zone adjacent to the pile (Poulos, 1988) or caused by non-linearity, will reduce the amount of interaction between piles.

An alternative way of viewing the reduced interaction, is to base all estimates of group response on the far-field, low-strain, stiffness of the soil. Any additional pile displacement that occurs due to higher strains in the vicinity of the pile, may be added in afterwards. Essentially, this approach is similar to that suggested by Focht and Koch (1973) for the treatment of group effects when considering lateral loading of piles. The approach is illustrated in Figure 15. For a single pile, a non-linear load transfer curve may be derived, for example assuming a hyperbolic stress-strain model for the soil. The initial tangent of the load transfer curve is G_0/ζ where G_0 is the initial shear modulus of the soil. The deviation (AB) from the initial tangent line is due to local strains.

The group pile response is constructed from the softened 'elastic' response, now with gradient G_0/ζ^* , to which is added the original 'plastic' displacements of the single pile. As discussed previously for single piles, the plastic component of displacement for the pile shaft will only rarely exceed the elastic component, and only at high mobilisation ratios of the pile shaft capacity.

It should be noted that, for many pile groups the efficiency due to elastic interaction will be 0.1 or less, implying softening of the single pile response by a factor in excess of 10. The addition of a small amount of plastic displacement (generally less than the elastic displacement of the original single pile) will be immaterial.

The relative non-linearity of a single pile and a typical group is illustrated in Figure 16, which shows the secant stiffness (normalised by the initial tangent stiffness) plotted against the degree of strength mobilisation. The two curves marked 'Base' and 'Shaft' are the 'element' responses, the former being a direct hyperbolic relationship (equation (14)), and the latter being the integrated form (equation (20), with $R_f = 1$ and $\zeta = 4$).

The curve for the single pile is taken from the RATZ fit to the load test data, shown in Figure 10. It is interesting to note that the combined shaft and base response results in a variation of secant stiffness which follows the basic hyperbolic relationship quite closely. This perhaps accounts for the success of Chin's (1970) approach for extrapolating pile load tests. The final curve represents a typical pile in a group of, say, 25 - 100 piles, where the elastic component of the shaft response has been softened by a factor of 10 (in the manner of Figure 15) and the base component has been softened by a factor of 2.5. In spite of more load being transferred to the base of the group pile, the response is considerably more linear than the single pile, until the load level exceeds about 70 % of the ultimate capacity.

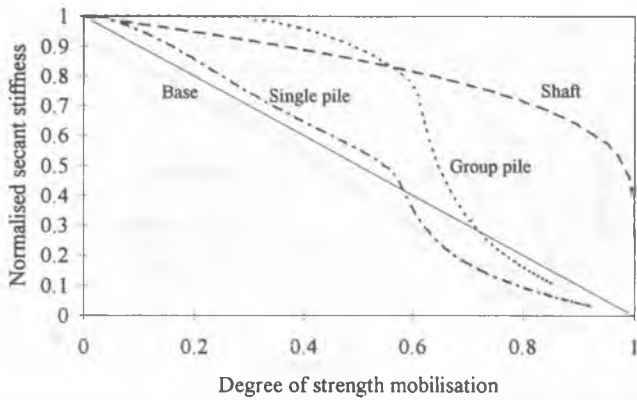


Figure 16 Comparison of non-linear response for single and group piles

While the conclusions from the above example will vary in detail depending on the relative proportion of load carried by shaft and base, and on the degree of interaction, it serves to illustrate the general effects of soil non-linearity. Overall, it may be concluded that non-linearity of the soil may be considered as having a relatively small effect on pile group response, provided that the group response is calculated correctly, using the initial tangent value of soil modulus. Only at very high mobilisation levels will the secant stiffness of the pile response start to drop.

A further example of the treatment of soil non-linearity is taken from Thorburn et al (1983), who describe the performance of piled foundations for storage tanks. Two sizes of tank were constructed, one of 12.5 m in diameter, supported by 55 piles, and one of 17.5 m in diameter, supported by 97 piles (see Figure 17). The piles were precast concrete, each 250 mm square, embedded 29 m and 32 m into alluvial silty clay with a strength profile approximated by $s_u = 6 + 1.8z$ kPa, where z is the depth in m.

Figure 18 shows the measured response of a 29 m long test pile that was loaded to failure, and the fitted response computed using the program, RATZ, assuming a shaft friction distribution of $\tau_s = 1.9z$ kPa, and a shear modulus of $G_0 = 1.5 + 0.45z$ MPa (Young's modulus of the piles was measured as 26 GPa). It may be noted that strain-softening effects limit the maximum pile load to just below 800 kN, compared with the theoretical capacity of 860 kN.

The piles for the tank foundation were laid out on a triangular grid at a spacing of 2 m. For the smaller tank (with 55 piles), values for the parameters ζ^* and ξ^* may be calculated for a typical pile as about 80 and 1.8 respectively. The resulting response of a typical pile in the group may then be calculated as shown in Figure 18.

At the working load level of 440 kN, the single pile showed about 6 mm displacement, although some creep movement was still observable. The calculated response for a typical group pile gives a displacement of 27 mm at working load. (A similar figure may be arrived at by considering an equivalent pier, with an equivalent Young's modulus of $E_{eq} = 500$ MPa.) This compares with measured settlements in the range 29 - 30 mm. The discrepancy may be explained in terms of small additional settlements arising from creep and the effects of load cycling from operation of the tanks (see the single load cycle during the pile test, Figure 18). As noted by Thorburn et al (1983), the direct use of elastic interaction factors would have led to a significant overestimate of the tank settlements.

Equivalent Pier Approach

In Section 2 of this paper, analytical approaches were discussed where the pile group was replaced either by an equivalent pier, of the same axial stiffness of the combined piles and soil, or an equivalent raft, situated part

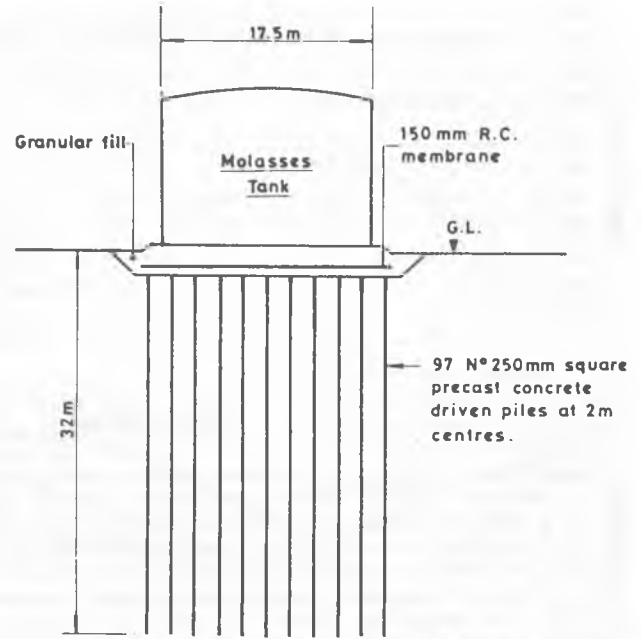


Figure 17 Pile layout for molasses storage tank (Thorburn et al, 1983)

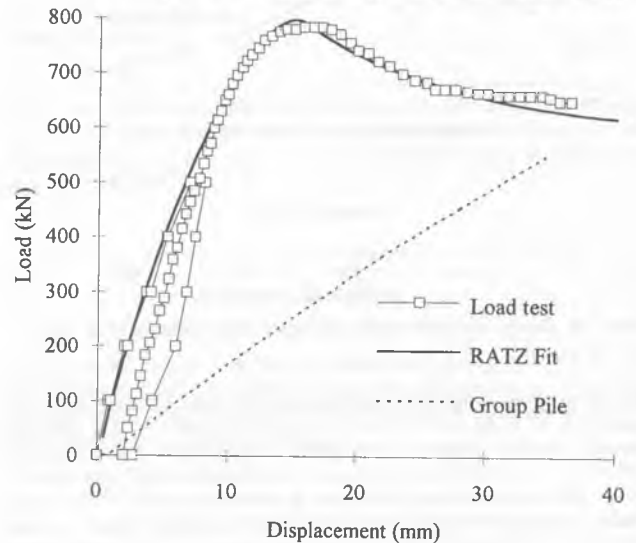


Figure 18 Measured and computed pile responses

way down the length of the piles. It was suggested that the aspect ratio of the pile group might indicate which of the two approaches should be preferred. In practice, there is a considerable region of overlap, where both approaches yield surprisingly accurate estimates of the pile group stiffness.

In order to assess the relative accuracy of these approaches, it is necessary to define an absolute standard for comparison. However, as commented earlier, enormous computational resources are needed to analyse the response of large groups of piles, and the commonly used approaches generally involve simplifications which lead to a consistent bias. As illustration of this, Figure 19 shows the computed overall pile groups stiffness for square groups of piles, with $l/d = 25$, $E_p/G = 1000$, $\nu = 0.5$. Three methods of estimating the pile group stiffness have been used, based on design charts available in the literature, which are also linked with commercially available computer codes:

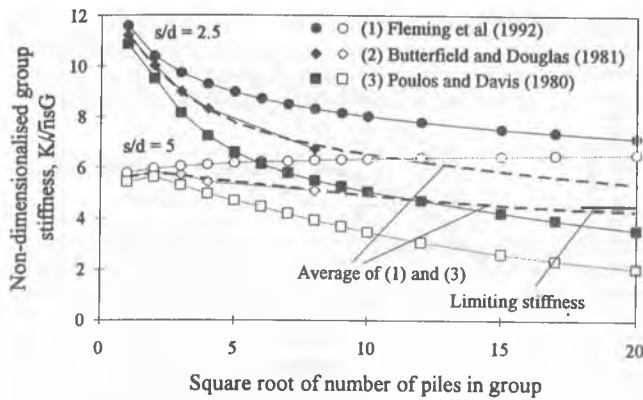


Figure 19 Comparison of different pile group analysis methods

- (1) The 'efficiency' approach described by Fleming et al (1992), based on analyses using the PIGLET program (Randolph, 1987).
- (2) The interaction factor approach of Poulos and Davis (1980), which is derived from analyses using the DEFPIG program (Poulos, 1980).
- (3) The charts of Butterfield and Douglas (1981), based on the full BEM solution incorporated in the PGROUP program (Banerjee and Driscoll, 1978).

Figure 19 shows the pile group stiffness, normalised as $k_p / (\sqrt{ns}G)$ as a function of the size of the pile group, for pile spacings of $s/d = 2.5$ and 5.0 . It may be seen that approaches (1) and (3) give divergent results, with the computed pile group stiffness differing by a factor of two or more for very large pile groups. The second, and most rigorous, approach falls close to the average of the other two approaches, but is limited to groups of only 64 piles.

For large pile groups, where the ratio of pile group width to pile length becomes much greater than unity, the pile group stiffness should approach

Table 3 Details of pile group and equivalent pier geometries

| Pile Group Details | | | | Equivalent Pier | | | |
|--------------------|-------|-----|------------------------------|-----------------|------------|------------|----------|
| ℓ/d | s/d | n | $R = \frac{\sqrt{ns}}{\ell}$ | k_p/dG | d_{eq}/d | E_{eq}/G | k_p/dG |
| 25 | 3 | 16 | 1.4 | 116 | 10.2 | 159 | 127 |
| 50 | 3 | 64 | 2.0 | 244 | 23.7 | 118 | 272 |
| 15 | 3 | 25 | 2.2 | 118 | 13.5 | 140 | 124 |
| 25 | 3 | 64 | 2.8 | 200 | 23.7 | 118 | 212 |
| 50 | 3 | 289 | 4.2 | 437 | 54.1 | 102 | 459 |
| 15 | 3 | 100 | 4.5 | 215 | 30.5 | 111 | 211 |
| 25 | 3 | 289 | 5.9 | 377 | 54.2 | 102 | 368 |
| 25 | 4 | 9 | 1.2 | 100 | 9.0 | 114 | 113 |
| 50 | 5 | 25 | 1.6 | 196 | 22.6 | 53 | 229 |
| 15 | 5 | 9 | 1.7 | 91 | 11.3 | 75 | 105 |
| 25 | 5 | 25 | 2.2 | 167 | 22.6 | 53 | 192 |
| 100 | 5 | 100 | 2.2 | 407 | 50.8 | 43 | 478 |
| 50 | 5 | 100 | 3.2 | 360 | 50.8 | 43 | 407 |
| 15 | 5 | 36 | 3.5 | 176 | 28.2 | 49 | 193 |
| 25 | 5 | 100 | 4.5 | 317 | 50.8 | 43 | 338 |
| 50 | 8 | 9 | 1.2 | 131 | 18.1 | 32 | 162 |
| 15 | 8 | 4 | 1.5 | 69 | 9.0 | 53 | 86 |
| 25 | 8 | 9 | 1.7 | 120 | 18.1 | 32 | 148 |
| 50 | 8 | 36 | 2.4 | 267 | 45.1 | 22 | 328 |
| 15 | 8 | 16 | 2.9 | 143 | 27.1 | 26 | 178 |
| 25 | 8 | 36 | 3.4 | 240 | 45.1 | 22 | 290 |
| 50 | 8 | 144 | 4.8 | 530 | 99.3 | 19 | 614 |

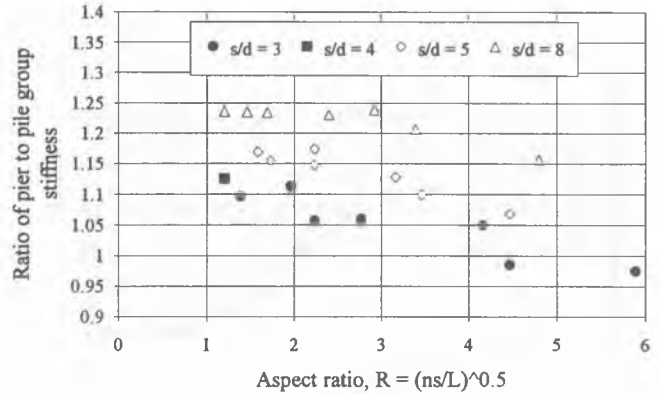


Figure 20 Ratio of equivalent pier stiffness to true pile group stiffness

that of a shallow foundation. This would correspond to a normalised stiffness of about 4.5 on Figure 19, as indicated. This limit is consistent with the trend in the results from Butterfield and Douglas, and with the average of the other two approaches. The average of those two approaches has therefore been used as a basis for assessing the accuracy of the equivalent pier method.

Poulos (1993) has presented the results of a parametric study, comparing the equivalent pier and raft methods with more rigorous analysis. The study was restricted to groups of up to 25 piles, with the widest aspect ratio of $[(\sqrt{n} - 1)s + d]/\ell = 0.52$. That study has been extended here to include pile groups of up to 289 piles, at spacings in the range $s/d = 3 - 8$, with overall geometry of the group having aspect ratios between 0.5 and 2. Details of the cases analysed are shown in Table 3, taking $E_p/G = 1,000$ and $\nu = 0.25$ throughout.

Figure 20 shows the ratio of pile group stiffness computed using (a) an equivalent pier approach and (b) using the pile group analysis program, PIGLET, plotted against the ratio $R = \sqrt{ns}/\ell$ (this provides the clearest trend in the results). The equivalent pier approach tends to overestimate the pile group stiffness for low values of R (surprisingly) and for high values of the spacing ratio, s/d (where the pile group is less stiff, since the soil between the piles is free to undergo significantly lower displacements). However, the accuracy of the equivalent pier approach is encouragingly high, even for large values of R , where the foundation would appear more as a relatively shallow region of reinforced soil. The ease of use of equation (16) (with the modified expression for ζ , equation (19)) renders it an attractive alternative to the use of charts or computer programs for estimating the average settlement of large pile groups.

Differential Settlement

The simplified approaches of an equivalent raft or an equivalent pier do not enable the differential settlement of a pile group to be calculated. This aspect of pile design has received relatively little attention, and yet it is an important issue, particularly where the main purpose of the piles is to limit structural damage caused by variation of settlement across the foundation.

It is convenient to express the differential settlement as a proportion of the average settlement of the foundation, with the latter being estimated using the methods described previously. For a shallow foundation of a given shape (in plan), the normalised differential settlement is a function only of the relative raft-soil stiffness, defined for a circular raft as (Brown, 1969)

$$K_{rc} = \frac{2(1 + \nu)E_r}{G} \left(\frac{t}{a}\right)^3 \quad (29)$$

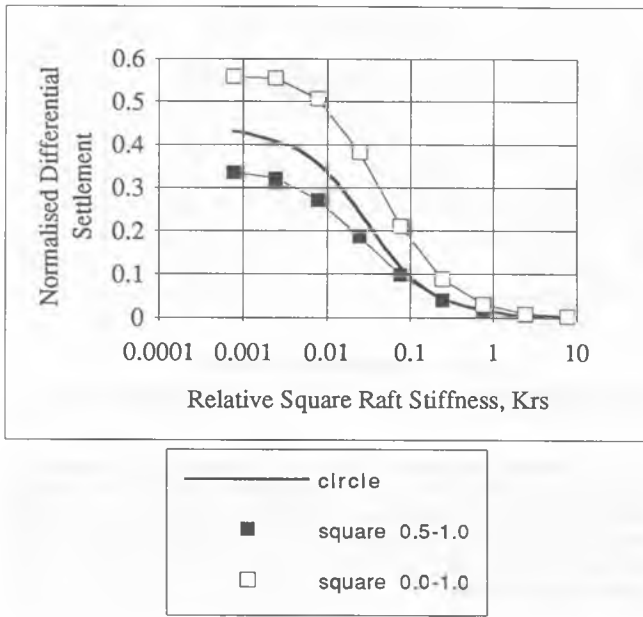


Figure 21 Normalised differential settlements as a function of raft stiffness

where E_r , t and a are respectively the Young's modulus, thickness and radius of the raft. An equivalent expression for a rectangular raft of breadth B , and length, L ($L > B$) has been proposed by Brown (1975), and is defined as

$$K_{rs} = \frac{2(1+\nu)E_r}{G} \frac{4B}{3\pi L} \left(\frac{t}{L}\right)^3 \quad (30)$$

For square rafts, it is convenient to define a co-ordinate system which varies along one edge from 0 at the corner, to 0.5 at the mid-side, and then progresses across the raft to a value of 1 at the centre (Clancy and Randolph, 1993). This co-ordinate system will be used to illustrate the pattern of differential settlements for square rafts.

Figure 21 shows the ratio of differential settlement to average (absolute) settlement for circular and square rafts, as a function of the relative raft stiffness, K_{rc} . The results for a square raft have been plotted for a raft of the same plan area as the circular raft (giving $L = B = \sqrt{\pi a}$). This equivalence gives $K_{rc} = 13.1K_{rs}$.

For pile groups, the picture of differential settlement is more complicated, since the relative magnitude is affected by the size of the group (n), the spacing ratio (s/d) and the slenderness ratio (ℓ/d). Randolph and Clancy (1993) have shown that the normalised differential settlement for square pile groups with a fully flexible pile cap may be expressed as a function of the quantity R (equation (6)). The resulting relationship between normalised differential settlement and R is approximately independent of the precise values of n , s/d or ℓ/d .

Figure 22 shows the variation of differential settlement, normalised by the average settlement, for square pile groups of varying size, all with stiffness ratio $E_p/G = 2500$. The piles are loaded uniformly (fully flexible pile cap). Particularly for long piles, the normalised differential settlement is a virtually unique function of R , increasing linearly from zero over the range $0 < R < 4$, and then, for $R > 4$, reaching a limit which is similar to that for a square raft foundation (see Figure 21). Thus, to a first approximation, the normalised differential settlement may be estimated from

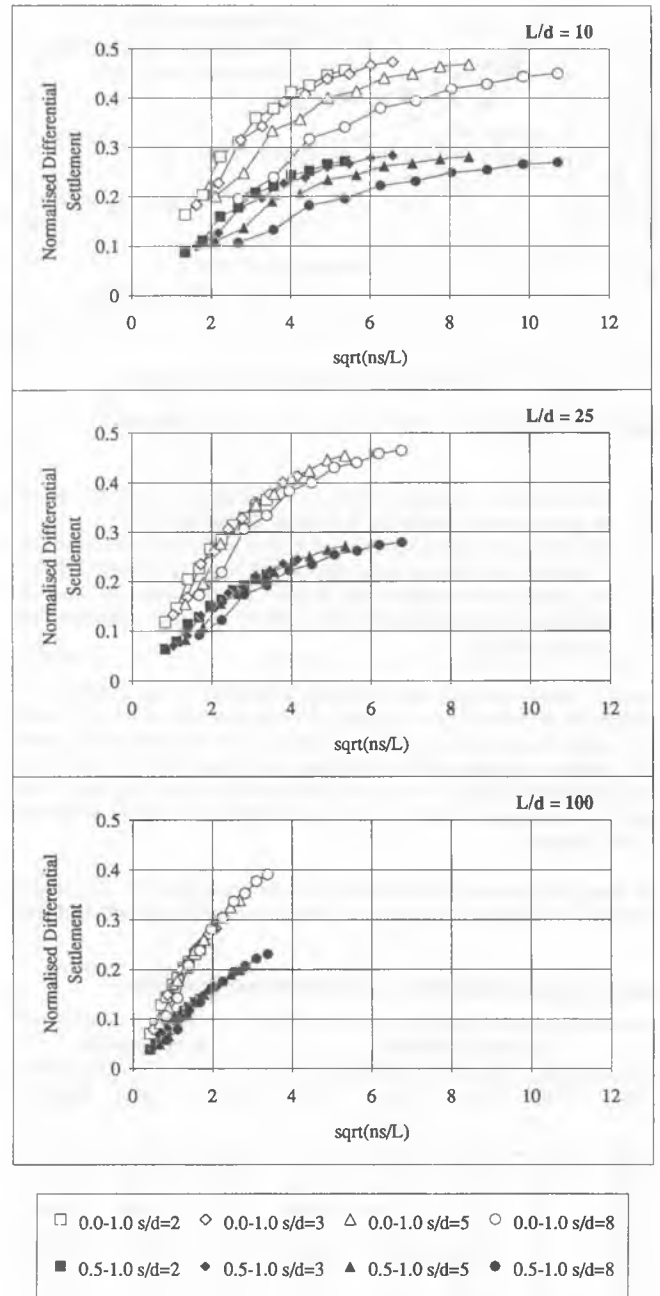


Figure 22 Differential settlements for pile groups, as a function of the ratio, R (after Randolph and Clancy, 1993)

$$\frac{\Delta w}{w_{avg}} \approx f \frac{R}{4} \quad \text{for } R \leq 4$$

$$\frac{\Delta w}{w_{avg}} \approx f \quad \text{for } R > 4 \quad (31)$$

where $f = 0.3$ for centre to mid-side, and $f = 0.5$ for centre to corner.

For pile caps of intermediate stiffness, the differential settlements will reduce, as for a raft foundation. Randolph and Clancy (1993) recommend that such pile groups be treated in a similar manner to a raft foundation.

The raft-soil stiffness ratio, K_{rs} , is used to determine the normalised differential settlement from curves such as in Figure 21, but modified to allow for the reduced maximum differential settlement (corresponding to a fully flexible pile cap) for pile groups where R is less than 4.

PILED RAFTS

In recent years, there has been a rapid increase in the number of piled raft foundations, particularly in stiff clay soils. Such soils offer reasonably good support for raft foundations, generally providing adequate bearing capacity for the structure, and yet excessive settlement may occur without the introduction of piles. Franke (1991) discusses the performance of four different piled rafts on Frankfurt clay, including the foundations for Europe's tallest building (see also Sommer, 1993). In each case, piles were used to limit settlements, the layout of the piles being chosen according to the distribution of structural load, in order to minimise bending effects in the raft.

The numerical approaches described in Section 2 offer sufficient flexibility to analyse virtually any geometry of pile group and raft, although published parametric studies have of necessity been limited to regular arrays of piles (for example, Hain and Lee, 1978; Bilotta et al, 1991). Key questions that arise in the design of piled rafts concern the relative proportions of load carried by raft and piles, and the effect of the additional pile support on absolute and differential settlements. These questions may be answered, at least approximately, through consideration of the response of each component (the raft, and the complete pile group) together with interaction between the components.

Adopting subscripts of p for the pile groups, and r for the raft (or pile cap), the settlement of each component may be expressed as (Randolph, 1983)

$$\begin{Bmatrix} w_p \\ w_r \end{Bmatrix} = \begin{bmatrix} 1/k_p & \alpha_{pr}/k_r \\ \alpha_{rp}/k_p & 1/k_r \end{bmatrix} \begin{Bmatrix} P_p \\ P_r \end{Bmatrix} \quad (32)$$

where α_{pr} and α_{rp} are interaction factors, and P and k are the loads and stiffnesses relating to each component. From the reciprocal theorem, the terms on the trailing diagonal of the flexibility matrix must be equal, so that the interaction factors are related by

$$\alpha_{pr} = \alpha_{rp} \frac{k_r}{k_p} \quad (33)$$

Since the (average) settlement of piles and raft are identical, the above two expressions allow the overall stiffness, k_{pr} , and the proportion of load carried by the raft to be calculated as:

$$k_{pr} = \frac{k_p + (1 - 2\alpha_{rp})k_r}{1 - \alpha_{rp}^2(k_r/k_p)} \quad (34)$$

and

$$\frac{P_r}{P_r + P_p} = \frac{(1 - \alpha_{rp})k_r}{k_p + (1 - 2\alpha_{rp})k_r} \quad (35)$$

For single piles with circular caps of radius r_c , Randolph (1983) has shown that the interaction factor, α_{rp} , may be approximated by

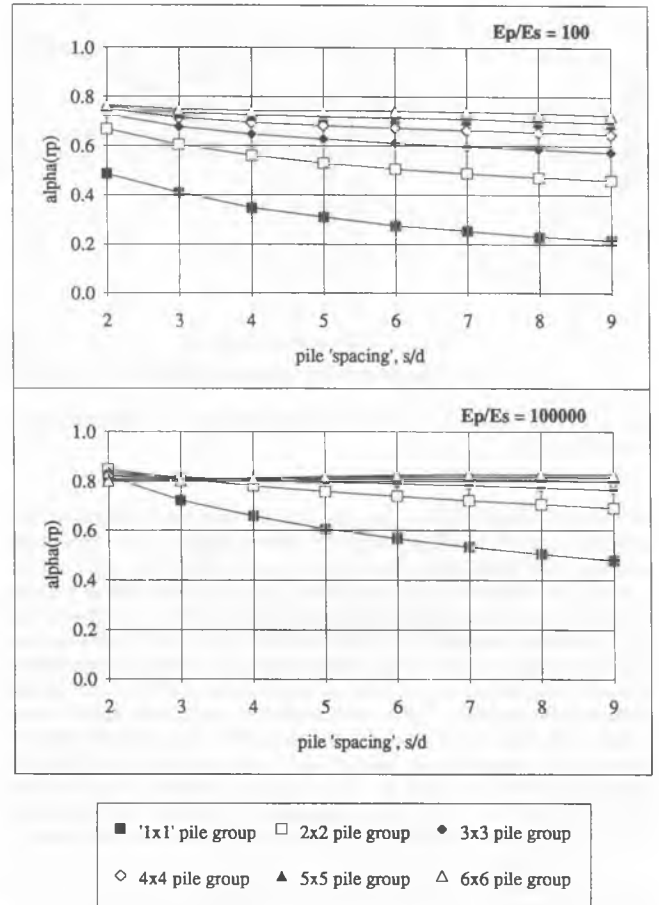


Figure 23 Values of interaction factor α_{rp} for groups of varying size (after Clancy and Randolph, 1993)

$$\alpha_{rp} = 1 - \frac{\ell n(r_c/r_o)}{\zeta} \quad (36)$$

In principle, this relationship may also be used for larger pile groups, where an equivalent radius, r_c , is calculated from the area of raft associated with each pile. However, more rigorous analyses reported by Clancy and Randolph (1993) show that, as the group size increases, the value of α_{rp} tends towards a constant value of about 0.8, independent of the pile spacing, slenderness ratio or stiffness ratio, as shown in Figure 23. This leads to an expression for the piled raft stiffness of

$$k_{pr} = \frac{1 - 0.6(k_r/k_p)}{1 - 0.64(k_r/k_p)} k_p \quad (37)$$

from which it may be seen that the combined stiffness of the foundation will be close to that of the pile group alone. Similarly, the ratio of loads carried by the pile cap (or raft) and the pile group is

$$\frac{P_r}{P_p} = \frac{0.2}{1 - 0.8(k_r/k_p)} \frac{k_r}{k_p} \quad (38)$$

which will typically lie in the range 0.3 - 0.5 times (k_r/k_p) .

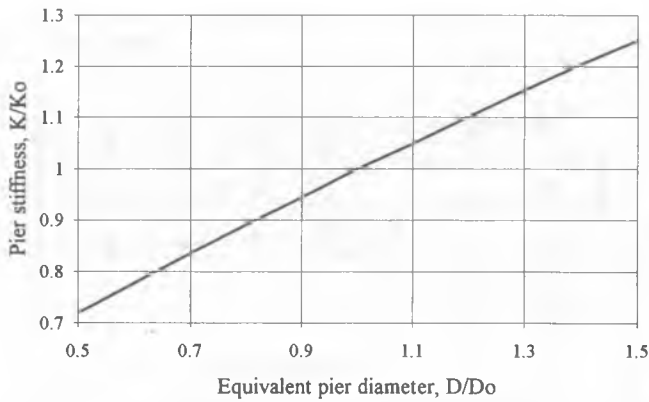


Figure 24 Variation of pier stiffness with diameter, for constant cross-sectional rigidity

The relatively small effect of the pile cap on the overall stiffness of the foundation may be anticipated from the relative accuracy of the equivalent pier approach. Essentially, the only modification needed for piled rafts is to extend the area of the equivalent pier to match the full area of the pile cap, rather than the area occupied by the piles themselves. Typically, this will increase the diameter of the equivalent pier by 10 - 20 %, although the total cross-sectional rigidity of the equivalent pier (which is determined primarily by the sum of the pile cross-sectional rigidities) will remain approximately constant. Under these conditions, for overall aspect ratios of pier in the range $0.5 < \ell/d_{eq} < 2$, the pier stiffness, k_p , (load divided by settlement) is approximately proportional to the square root of the pier diameter, as shown in Figure 24. Thus, for a pile cap that extends beyond the outer piles by 20 % of the foundation dimension, the combined stiffness of the piled raft will be 10 % greater than that of the pile group.

Design Philosophy

One of the principle benefits of casting a pile cap directly on the ground is in enforcing a 'block' type failure. As noted by Franke (1991), the mode of failure of piles within a large group is very different from that of a single pile, even where the pile cap is suspended above the ground. Due to interaction effects, slip between the soil and piles within a group will tend to start at the base of each pile and progress upwards, rather than vice versa for a single pile. If the pile cap acts directly on the soil surface, relative slip between pile and soil cannot occur at shallow depths, and the ultimate limit state must involve punching failure of the entire block of soil containing the piles.

Three different design approaches may be identified for piled rafts:

(1) *Conventional*. What may be termed the 'conventional' approach is one where the foundation is designed essentially as a pile group, with regular spacing of the piles over the complete foundation area, but where allowance is made for the load transmitted directly from the pile cap to the ground. The analysis of this case follows that outlined above (for example, equations (37) and (38), or an equivalent pier analogue), and the principal benefit is a reduction in the total number of piles, due to perhaps only 60 - 75 % of the total structural load being carried by the piles.

One of the best documented case histories of the performance of a piled raft of this type has been described by Cooke et al (1981). Although the foundation was designed essentially as a standard pile group, with over 350 piles installed on a rectangular grid at a spacing of 3.6 diameters, subsequent analyses, validated by detailed measurements of performance, have suggested that the number of piles could have been reduced to less than 100, with only marginal increase in average settlement (Padfield and Sharrock, 1983; Randolph and Clancy, 1993).

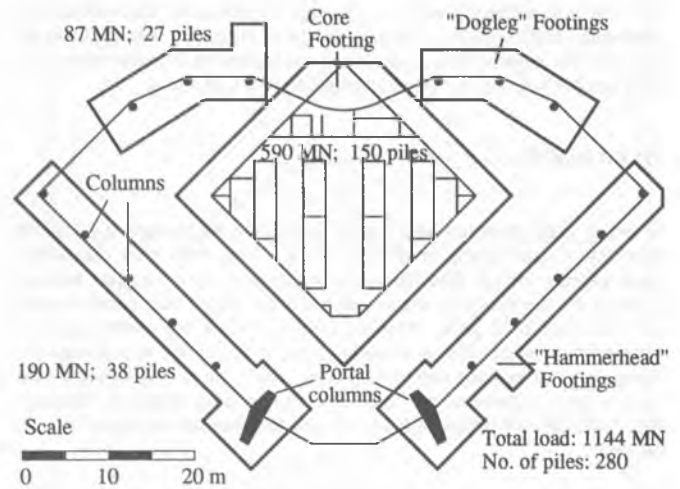


Figure 25 Foundations for QV1 building (Smith and Randolph, 1990)

A case history with a more complex foundation layout has been presented by Smith and Randolph (1990). Five independent units, each consisting of a raft supported by piles, formed the foundation of the QV1 building in Perth (see Figure 25). The piles were 0.8 m in diameter by 20 m long, cast in situ under bentonite, and load tests indicated minimum shaft capacities of around 3.5 MN, beyond which the secant stiffness of the pile head response dropped rapidly. The total structural load of 1144 MN was carried by 280 piles, with an estimated average working load per pile of around 3 MN, after allowing for over 25 % of the load transmitted directly from the pile cap to the ground. Clancy (1993) has carried out a full numerical analysis of the foundation, and obtained good agreement with the measured settlements, which ranged from 40 mm at the centre to 17 mm at the extreme corners.

As pointed out by Hooper (1979) and Cooke (1986), relatively few piles are required to establish a region of reinforced soil with a high equivalent Young's modulus, and adding further piles within that region is unproductive in terms of reducing settlements. The equivalent pier approach may be used, in conjunction with the closed form expression for pile stiffness in equation (16), to estimate optimum pile densities beyond which there is negligible elastic compression of the pier.

For very stiff piles, equation (16) reduces to

$$\frac{P_t}{G_\ell r_o w_t} = \frac{4\eta}{(1-\nu)\zeta} + \rho \frac{2\pi \ell}{\zeta r_o} \quad (39)$$

This expression applies for single piles where $\ell/d < 0.25 \sqrt{E_p/G_\ell}$. For an equivalent pier, which is much stubbier and where the parameter ζ is generally closer to 2 than 4, the limit is $\ell/d_{eq} < 0.1 \sqrt{E_{cq}/G_\ell}$.

An interesting case study in the use of a few, widely spaced, piles has been presented by Yamashita et al (1993). A total of only 20 piles, 16 m long and varying in diameter between 0.7 m and 0.8 m, were installed directly beneath the columns of a building of plan area 23 m by 24 m. The relevant equivalent pier has diameter 26.5 m and Young's modulus 700 MPa. From the soil modulus values quoted by Yamashita et al (1993), a shear modulus profile of $G = 6 + 2z$ MPa is appropriate. This gives $\ell/d_{eq} = 0.14 \sqrt{E_{cq}/G_\ell}$, which is close to the limit where further internal piles would have little influence on the overall foundation stiffness. The equivalent pier stiffness may be computed as 3500 MN/m (compared with that for a rigid pier of 3900 MN/m), which compares with reported average settlements of about 12.5 mm for a total structural load of 47.5 MN (stiffness of 3800 MN/mm).

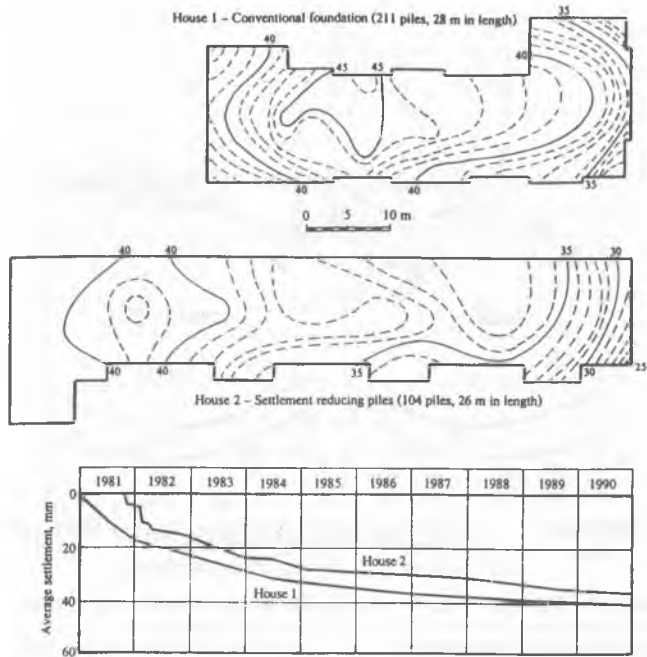


Figure 26 Settlement performance of two buildings, one on conventional piles and one on creep piles (after Hansbo, 1993)

(2) *Creep Piling*: So-called 'creep piling' has been proposed by Hansbo and Källström (1983), with case histories described in detail by Hansbo and Jendeby (1983) and Jendeby (1986). The two principles behind the original approach (for relatively soft cohesive soils) are:

- each pile is designed to operate at a working load at which significant creep starts to occur, typically at about 70 - 80 % of its ultimate bearing capacity;
- sufficient piles are included to reduce the net contact pressure between raft and soil to below the preconsolidation pressure of the clay.

Essentially the foundation is designed as a raft foundation, but the total settlement is reduced in the manner suggested by Burland et al (1977), by the inclusion of piles, distributed uniformly beneath the raft, that are allowed to move plastically relative to the surrounding soil. The choice of the creep load as the working load of each pile prevents high loads developing in piles at the edges of the foundation, allowing more precise determination of bending moments in the raft. Figure 26 compares settlement performance of two buildings, one on conventional piles and one on creep piles (Hansbo, 1993). There is clearly a major saving in piling costs for the second building, with little difference in performance.

The approach has also been explored for non-cohesive soil (Hansbo, 1993; Phung, 1993), and it has been shown that the effective stress increase due to load transmitted from the pile cap leads to an increase in the capacity of the supporting piles. Essentially, the piles will operate below their (enhanced) creep load, and the performance of the foundation may be analysed by the conventional means described earlier.

(3) *Differential Settlement Control*: The two approaches above adopt a uniform distribution of piles beneath the raft, with the primary aim being to limit absolute settlements to an acceptable amount. Differential settlements will be reduced as a consequence of lower total settlements. However, a more direct approach is to design the pile support in such a way as to minimise differential settlements at the outset, without necessarily reducing the average settlement significantly.

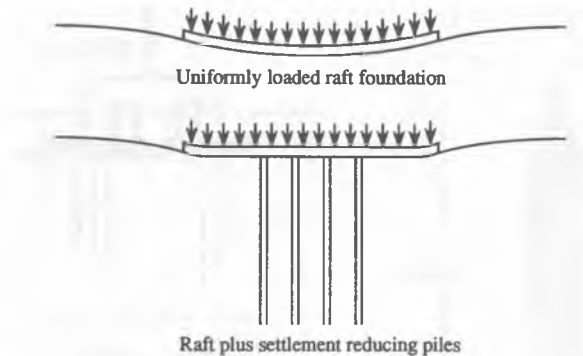
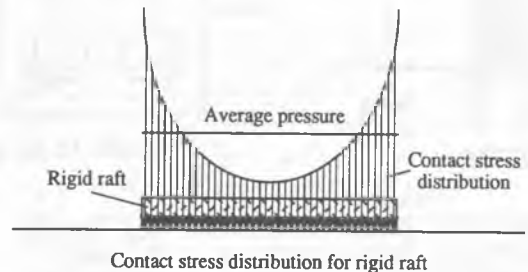
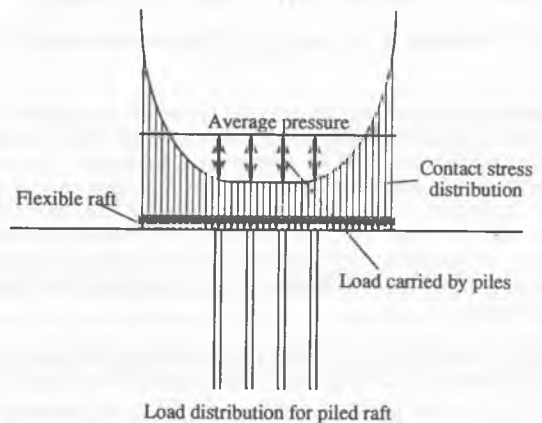


Figure 27 Central piles to reduce differential settlement



Contact stress distribution for rigid raft

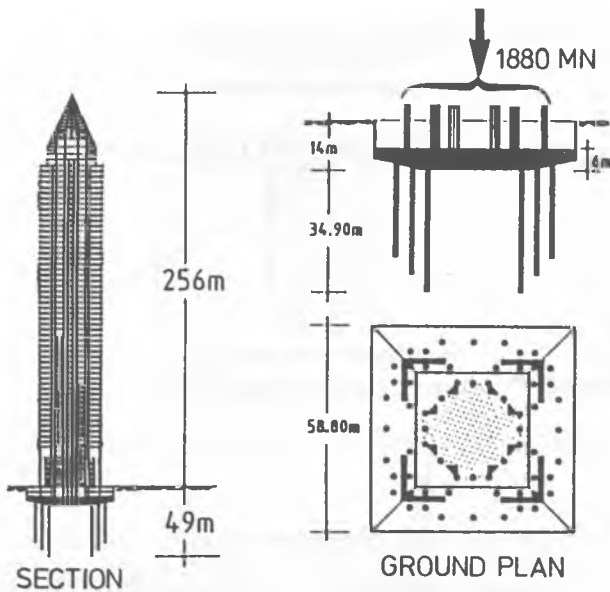


Load distribution for piled raft

Figure 28 Schematic design approach for settlement reducing piles

For conventional piled rafts, where the major portion of the load is carried by the piles, the geometry will tend to be such that the overall aspect ratio of the foundation exceeds unity, and the parameter R (equation (6)) will generally exceed 3. As such, the normalised differential settlement can be expected to be similar to those for a comparable raft foundation. Effectively, as discussed by Clancy and Randolph (1993), the absolute differential settlements are obtained from an analysis of the raft alone, but factored by the ratio k_r/k_{pr} , to account for the overall reduction in settlements due to the presence of the piles in the complete foundation. Typical raft stiffness ratios generally lie in the range $0.01 < K_{RS} < 0.1$, giving differential settlements, as a proportion of the average settlement, in the range 10 - 30 % (centre to mid-side) and 20 - 50 % (centre to corner) as shown in Figure 21.

Figures 27 and 28 show schematically the principles behind the design of piles to reduce differential settlements. Assuming that the structural load is relatively uniformly distributed over the plan area of the building, then there will be a tendency for an unpiled raft to 'dish' in the centre. A few piles added over the central region of the foundation, probably loaded to close to their ultimate capacity, will reduce that tendency, and thus minimise differential settlements.



64 PILES ϕ 1.30m
 28 PILES : 26.9m (EXTERNAL PILE RING)
 20 PILES : 30.9m (MIDDLE PILE RING)
 16 PILES : 34.9m (INTERNAL PILE RING)

Figure 29 Foundations of the MesseTurm (Thaher and Jessberger, 1991)

The required pile support may be estimated by consideration of the 'ideal' contact pressure distribution that acts beneath a rigid raft, where the central pressure is approximately half the average applied pressure. The central piles should thus be designed to absorb 50 - 70 % of the average applied pressure, leading to a contact pressure distribution for a flexible raft that matches that for a rigid raft, and will thus give minimal differential settlements. (Note that the piles themselves will contribute some settlement, and hence the piles should be designed to carry rather more than half the applied pressure.)

The idea of central piles to reduce both differential settlements and bending moments is in keeping with a scheme proposed by Padfield and Sharrock for the case history of the Cooke et al (1981), but contrasts with piling schemes adopted for the MesseTurm in Frankfurt (Sommer et al, 1991; Sommer, 1993) and explored at model scale by Thaher and Jessberger (1991). Those schemes have tended to concentrate piles towards the edges of the foundation, and thus run the risk of accentuating differential settlements unless an extremely thick raft is adopted (which must then carry high bending moments).

Figure 29 shows the foundation scheme for the MesseTurm. While the central ring of piles is longer than the outer ring (and thus provides greater support towards the centre where it is most needed), there is a complete lack of support in the central region of the foundation. Settlement profiles at building completion and 18 months later are shown in Figure 30 (Sommer et al 1991). In spite of the massively thick raft (6 m in the centre), significant differential settlements were observed. Additionally, measurement of contact pressures beneath the raft indicated central values of about 260 kPa (compared with average applied pressure of 540 kPa), but values in the outer region of less than 200 kPa (Sommer et al, 1991).

Example Application

In order to illustrate the principles discussed above, an example foundation will be analysed, consisting of a 36 m square raft subjected to an average

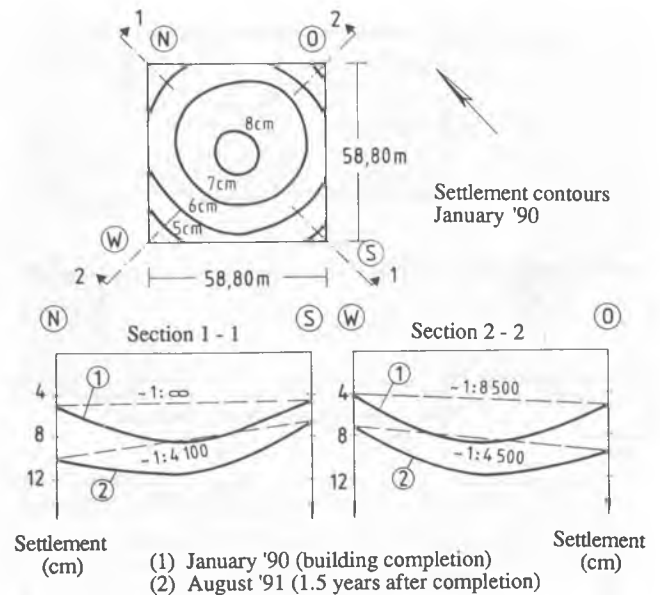


Figure 30 Measured settlements of the MesseTurm (Sommer et al, 1991)

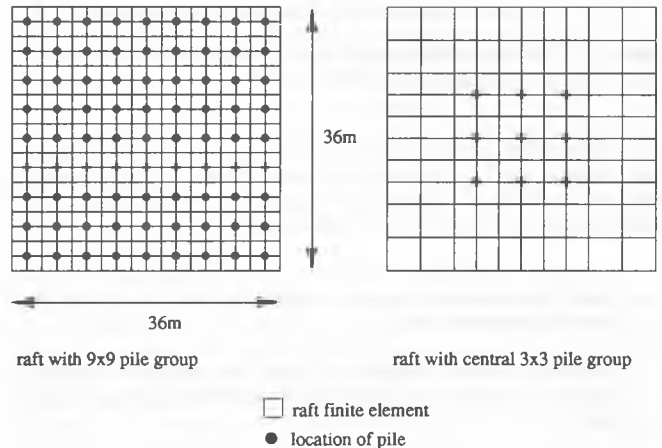


Figure 31 Foundation layouts for example application

loading of 600 kPa (total load of 780 MN). Figure 31 shows the foundation layout, with two different piling arrangements. The first consists of a 9 x 9 grid of piles at 4 m spacing, with other properties as given in Table 4 below.

The raft stiffness (assuming a rigid raft) may be calculated from (Poulos and Davis, 1974)

$$k_r = \frac{2.25GB}{(1-\nu)} = 13.5 \text{ MN/mm} \quad (40)$$

Table 4 Soil, pile and raft properties for example application

| | Soil | | Pile | | | Raft | |
|-------|------|-----|--------|-------|-----|----------|------|
| G | 100 | MPa | E_p | 35000 | MPa | L | 36 m |
| ν | 0.4 | | ℓ | 20 | m | B | 36 m |
| | | | d | 0.8 | m | K_{rs} | 0.01 |

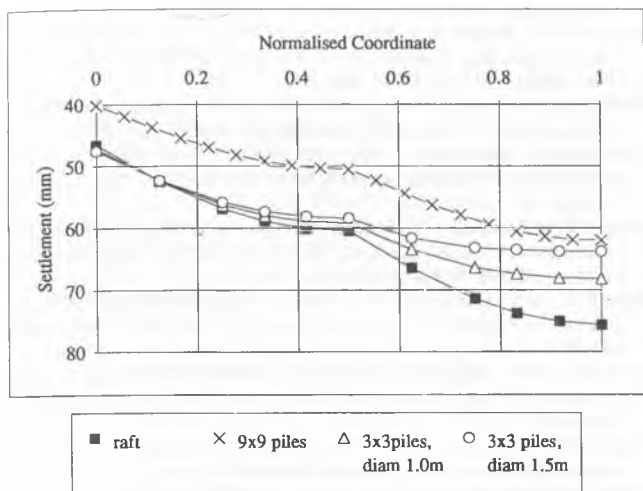


Figure 32 Settlement profiles for different pile layouts

The stiffness of the pile group may be estimated from an equivalent pier of diameter 36 m (equivalent in area to the 32 m wide pile group) and Young's modulus 1660 MPa, giving $k_p = 16.2$ MN/mm. Equations (37) and (38) then give an overall stiffness of the piled raft of 17.4 MN/mm, with 67 % of the load carried by the pile group. A direct calculation of the piled raft stiffness using an equivalent pier of diameter 40.6 m, and Young's modulus of 1370 MPa, leads to a stiffness of 17.5 MN/mm, which is consistent with the value obtained from the component stiffnesses.

The ratio R for the pile group (equation (6)) is 4, and hence differential settlements may be estimated with adequate accuracy from those for a purely raft foundation. For the relative raft stiffness of $K_{RS} = 0.01$, Figure 21 would indicate normalised differential settlements of 26 % (mid-side to centre) and 49 % (corner to centre). For an applied (average) vertical stress of 600 kPa, this would lead to an average settlement of the piled raft of 44 mm, and differential settlements of 12 mm between mid-side and centre, and 22 mm between corner and centre. A full numerical analysis yields identical differential settlements, but an average settlement some 18 % higher, at 52 mm (see Figure 32).

The second arrangement of piles consists of a 3 x 3 group, at a spacing of 6 m, situated over the central region of the raft. The pile length has been increased to 30 m, and the diameter to either 1 m, or 1.5 m. For a limiting shaft friction of 125 kPa, and end-bearing of 2 MPa, the ultimate pile capacity is 13.4 MN for the 1 m diameter, and 21.2 MN for the 1.5 m diameter pile. Assuming that some 80 % of the pile capacity is mobilised under working conditions, the effective pressure carried by the piles over the central region is then about 300 kPa and 470 kPa respectively, which correspond to 50 % and 80 % of the applied pressure.

Figure 32 shows settlement profiles, under the uniformly distributed working load of 780 MN, for the four cases of:

- (1) raft alone;
- (2) fully piled (9 x 9) raft, with raft-soil stiffness of $K_{RS} = 0.01$;
- (3) central 3 x 3 pile group, 1 m diameter, fully flexible pile cap;
- (4) central 3 x 3 pile group, 1.5 m diameter, fully flexible pile cap.

As anticipated, the central piles have little effect on the corner and edge settlements, and indeed reduce the average settlement by less than 5 %. However, their effectiveness in reducing differential settlements is evident. By contrast, the fully piled raft reduces the average settlement by 20 %, but shows virtually no change in differential settlements compared with the unpiled raft, apart from a slight reduction due to the pile cap stiffness.

The effectiveness of the central piles in reducing differential settlements is

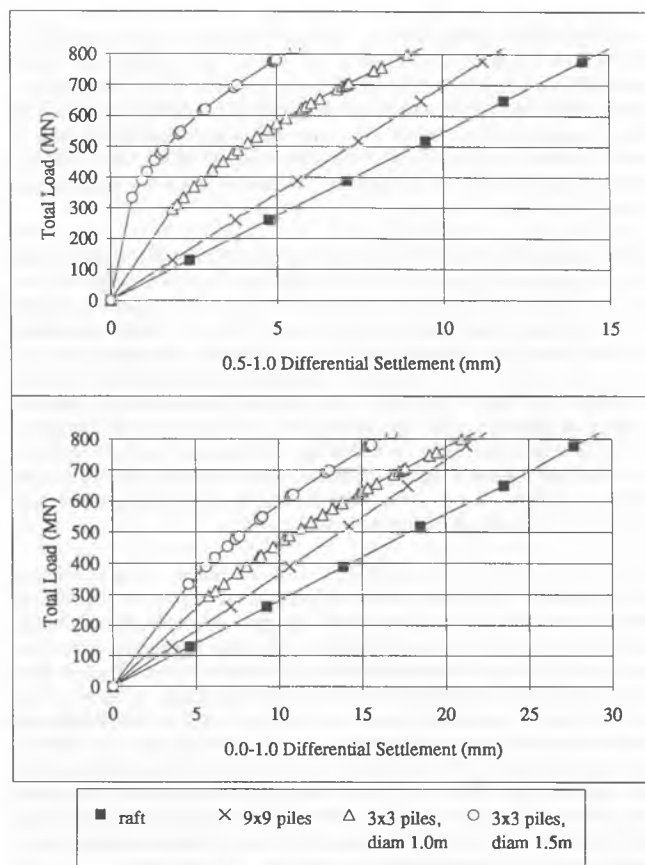


Figure 33 Development of differential settlements with load level

seen more clearly in Figure 33. The upper plot shows that the larger diameter central piles practically eliminate mid-side to centre differential settlements at low load levels. Even at the working load of 780 MN, when the capacity of the central piles is nearly fully mobilised, the differential settlements are reduced by a factor of 3 compared with the unpiled raft.

Differential settlements between the corner and the centre of the raft are reduced by the central piles, although the value of 15 mm for the case of 1.5 m diameter piles is still over 50 % of the value for the unpiled raft (28 mm). In practice, stiffening of the raft towards the corners due to the superstructure will help reduce such differential settlements further.

CONCLUSIONS

The science of pile design has advanced dramatically over the last twenty years, with greatly improved understanding and quantification of the effects of pile construction methods, of the stress changes that occur during pile installation and loading, of the manner of load transfer for single piles and pile groups and of interaction effects. This paper has concentrated on advances in design approaches for estimating the settlement performance of pile groups and piled rafts, with the principal aim being to provide simple analogue models which will allow engineers to optimise the required quantity and location of pile support.

Pile design is still centred primarily around the axial capacity of isolated piles, and the settlement performance at the nominal working load (total load divided by the number of piles). The performance of the complete group is then assessed through the use of interaction factors and group efficiencies derived from elastic theory. For this approach to be accurate,

due attention must be paid to the non-linear response of the soil. It has been argued that, at least in respect of load transferred from the pile shaft, the shear stress level in the bulk of the soil is such that the low strain modulus is appropriate. Thus the 'elastic' response of the pile within a group, including all interaction effects, should be calculated using the initial tangent modulus of the soil. Any additional displacement, due to local high shear strains adjacent to the pile, may be added later, although for most conventional pile groups the non-linear effects are insignificant except at very high load levels.

Sophisticated numerical techniques are now readily available to analyse the detailed response of pile foundations, including the effects of bending of the pile cap. The majority of these techniques are based on elastic interaction between each pile and raft element. However, such calculations are computationally intensive, and must generally be limited to relatively small pile groups. An alternative approach, which appears to offer comparable accuracy, is to consider the area occupied by the pile group as a region of reinforced soil. Essentially, the pile-reinforced soil is replaced by an equivalent pier, or by an inclusion of transversely isotropic soil with an enhanced vertical Young's modulus. This approach enables simple hand-calculations of pile group stiffness and load sharing between pile group and overlying raft to be performed.

The primary aim of pile foundations in many situations is that of limiting the settlement, particularly differential settlement across the foundation which is the main source of structural damage. While traditional design methods have aimed to minimise the absolute settlement, and thus automatically limit differential settlement, a more efficient approach is to minimise differential settlement directly, by appropriate location of the pile support. In general, depending on the precise distribution of structural loading, this will require the main pile support to be located towards the centre of the foundation, preventing the normal tendency for the foundation to dish in the centre. An example calculation has shown that, even for a fully flexible raft, a few piles located at the centre of the raft can reduce differential settlements by a factor of two, compared with a conventional pile group extending beneath the complete raft.

In many countries, there is current pressure to move towards a limit state design philosophy for pile foundations, with emphasis on the ultimate capacity and settlement performance of individual piles. However, the load transfer from a pile within a group is markedly different from that for a single pile, particularly where the pile cap rests directly on competent bearing ground. There is therefore a need to shift the emphasis in design more towards the global response of the foundation. For piled rafts, the ultimate state is one where the complete foundation punches into the soil, and the individual capacity of each pile is of little concern. Similarly, serviceability calculations will be carried out with greatest confidence by a new generation of analytical methods that treat the pile-soil composite as a whole, rather than attempt to model the detailed interaction between each foundation element.

REFERENCES

Aldridge, T.R. and Schnaid, F. 1992. Degradation of skin friction for driven piles in clay. *Proc. Conf. on Recent Large Scale Fully Instrumented Pile Tests in Clay*, ICE, London.

Baldi, G., Bellotti, R., Ghionna, V.N., Jamiolkowski, M. and Lo Presti, D.C.F. 1989. Modulus of sands from CPTs and DMTs. *Proc. 12th Int. Conf. on Soil Mech. and Found. Eng.*, Rio de Janeiro, Vol. 1: 165-170.

Banerjee, P.K. and Butterfield, R. 1981 *Boundary Element Methods in Engineering Science*, McGraw-Hill.

Bilotta, E., Caputo, V. and Viggiani, C., 1991. Analysis of soil-structure interaction for piled rafts. *Proc. 10th Europ. Conf. on Soil Mech. and Found. Eng.*, Florence: Vol. 1: 315-318.

Brown, P.T. 1969. Numerical analyses of uniformly loaded circular rafts on deep elastic foundations. *Geotechnique* 19: 301-306.

Brown, P.T. 1975. Strip footing with con-centrated loads on deep elastic

foundations. *Geotechnical Engineering* 6: 1-13.

Burland, J.B., Broms, B.B. and de Meillo, V.F.B. 1977. Behaviour of foundations and structures. *Proc. 9th Int. Conf. on Soil Mech. and Found. Eng.*, Tokyo: Vol. 2: 495-546.

Butterfield, R. and Banerjee, P.K. 1971. The elastic analysis of compressible piles and pile groups. *Geotechnique* 21(1): 43-60.

Butterfield, R. and Douglas, R.A. 1981. Flexibility coefficients for the design of piles and pile groups. *CIRIA: Technical Note 108*, London, CIRIA.

Carter, J.P. and Kulhawy, F.H. 1988. Analysis and design of drilled shaft foundations socketed into rock, *Report to Electric Power Research Institute, EL-5918*, Research Project 1493-4.

Chin, F.K. 1970. Estimation of the ultimate load of piles from tests not carried to failure. *Proc. 2nd. SE Asian Conf. Soil Eng.*, Singapore, 81-92.

Chin, F.K. 1972. The inverse slope as a prediction of ultimate bearing capacity of piles, *Proc. 3rd SE Asian Conf. Soil Eng.*, Hong Kong, 83-91.

Chow, Y.K. 1986. Analysis of vertically-loaded pile groups. *Int. J. Num. & Anal. Methods in Geomechanics*, 10(1): 59-72.

Cooke, R.W. 1986. Piled raft foundations on stiff clays - a contribution to design philosophy. *Geotechnique* 36(2): 169-203.

Cooke, R.W., Bryden-Smith, D.W., Gooch, M.N. and Sillett, D.F. 1981. Some observations of the foundation loading and settlement of a multi-storey building on a piled raft foundation in London clay. *Proc. ICE*, London: 107(Part 1), 433-460.

Clancy, P. 1993. *Numerical analysis of piled raft foundations*. Forthcoming PhD Thesis, The University of Western Australia.

Clancy, P. and Randolph, M.F. 1993. Analysis and design of piled raft foundations. Accepted for publication in *Int. J. Num. & Anal. Methods in Geomechanics*.

Fahey, M. and Carter, J.P. 1993. A finite element study of the pressuremeter test in sand using a non-linear elastic plastic model. *Can. Geot. J.*, April 1993.

Fleming, W.G.K. 1992. A new method for single pile settlement prediction and analysis. *Geotechnique* 42(3): 411-425.

Fleming, W.G.K., Weltman, A.J., Randolph, M.F. and Elson, W.K. 1992. *Piling Engineering (2nd Edition)*, Surrey University Press.

Focht, J. and Koch, K. 1973. Rational analysis of the lateral performance of pile groups. *Proc. 4th Ann. Offshore Tech. Conf.*, Houston.

Fox, L. 1948. The mean elastic settlement of a uniformly loaded area at a depth below the ground surface. *Proc. 2nd Int. Conf. Soil Mech. and Found. Eng.*, Vol. 1, 129.

Frank, R.A. 1974. Etude theorique du comportement des pieux sous charge verticale: Introduction de la dilatacion, *Rapport de Recherche No. 46*, Laboratoire Central des Ponts et Chaussées, Paris.

Franke, E. 1991. Measurements beneath piled rafts. *ENPC Conf. on Deep Found.*, Paris.

Goosens, D. and Van Impe, W.F. 1991. Long term settlements of a pile group foundation in sand, overlying a clayey layer. *Proc. 10th Europ. Conf. on Soil Mech. and Found. Eng.*, Florence, 1, 425-428.

Griffiths, D.V., Clancy, P. and Randolph, M.F. 1991. Piled raft foundation analysis by finite elements. *Proc. 7th Int. Conf. on Computer Methods and Advances in Geomechanics*, Cairns: 2, 1153-1157.

Hain, S.J. and Lee, I.K. 1978. The analysis of flexible pile-raft systems. *Geotechnique* 28(1): 65-83.

Hansbo, S. 1993. Interaction problems related to the installation of pile groups. *Proc. of 2nd Int. Geot. Sem. on Deep Foundations on Bored and Auger Piles*, Ghent, 59-66.

Hansbo, S. and Källström, R. 1983. A case study of two alternative foundation principles. *Väg-och Vattenbyggaren* 7-8: 23-27.

Hansbo, S. and Jendeby, L. 1983. A case study of two alternative foundation principles: conventional friction piling and creep piling. *Väg-och Vattenbyggaren* 7-8: 29-31.

Hardin, B.O. and Black, W.L. 1968. Vibration modulus of normally consolidated clay. *J. of the Soil Mech. and Found. Div, ASCE* 95(SM6): 1531-1537.

Hooper, J.A. 1979. Review of behaviour of piled raft foundations. *CIRIA Report 83*, Construction Industry Research and Information Association, London.

- Imai, T. and Tonouchi, K. 1982. Correlation of N value with S-wave velocity and shear modulus. *Proc. Europ. Symp. on Penetration Testing 2*, Amsterdam, 1, 67-72.
- Jardine, R.J., Potts, D., Fourie, A.B. and Burland, J.B. 1986. Studies of the influence of non-linear stress-strain characteristics in soil-structure interaction. *Geotechnique* 36(3): 377-396.
- Jendebly, L. 1986. *Friction piled foundations in soft clay. A study of load transfer and settlements*. Department of Geotechnical Engineering, Chalmers Univ. of Technology, Gothenburg. Dissertation.
- Kagawa, T. 1992. Moduli and damping factors of soft marine clays. *J. Geot. Eng. Div., ASCE* 118(9): 1360-1375.
- Kraft, L.M., Ray, R.P. and Kagawa, T. 1981. Theoretical t-z curves. *J. Geot. Eng. Div., ASCE* 107(11): 1543-1561.
- Lo Presti, D.C.F., Jamiolkowski, M. and Favazzi M. 1991. Maximum shear modulus measurements using bender elements during oedometer test. *Experimental Characterization and Modelling of Soils and Soft Rocks*, University of Naples, 99-112.
- Mindlin, R.D. 1936. Force at a point in the interior of a semi-infinite solid. *Physics* 7: 195-202.
- O'Neill, M.W., Ghazzaly, O.I. and Ha, H.B. 1977. Analysis of three-dimensional pile groups with non-linear soil response and pile-soil-pile interaction. *Proc. 9th Ann. Offshore Tech. Conf.*, Houston, Paper OTC 2838, 245-256.
- Onsaki, Y. and Iwasaki, R. 1973. On dynamic shear moduli and Poisson's ratios of soil deposits. *Soils and Foundations*, Vol. 13, No. 4.
- Padfield, C.J. and Sharrock, M.J. 1983. Settlement of structures on clay soils. *CIRIA: Special Publication 27*.
- Phung, D.L. 1993. *Footings with settlement-reducing piles in non-cohesive soil*. Department of Geotechnical Engineering, Chalmers Univ. of Technology, Gothenburg. Dissertation.
- Poulos, H.G. 1968. Analsis of the settlement of pile groups. *Geotechnique*, 18: 449-471.
- Poulos, H.G. 1993. An approximate numerical analysis of pile-raft interaction. Submitted for publication in *Int. J. Num. & Anal. Methods in Geomechanics*.
- Poulos, H.G. 1993. Settlement prediction for bored pile groups. *Proc. of 2nd Int. Geot. Sem. on Deep Foundations on Bored and Auger Piles*, Ghent, 103-117.
- Poulos, H.G. 1988. Modified calculation of pile-group settlement interaction. *J. Geot. Eng. Div., ASCE* 114(6): 697-706.
- Poulos, H.G. 1979. Settlement of single piles in non-homogenous soil. *J. Geot. Eng. Div., ASCE*, Vol. 105, No. GT5, 627-641.
- Poulos, H.G. 1989. Twenty-ninth Rankine Lecture: Pile behaviour-theory and application, *Geotechnique* 39(3): 363-415.
- Poulos, H.G. and Davis, E.H. 1974. *Elastic solutions for soil and rock mechanics*. Wiley.
- Poulos, H.G. and Davis, E.H. 1980. *Pile foundation analysis and design*. Wiley.
- Poulos, H.G. and Davis, E.H. 1968. The settlement behaviour of single axially-loaded incompressible piles and piers, *Geotechnique* 18(3): 351-371.
- Randolph, M.F. 1983. Design of piled raft foundations. *Proc. Int. Symp. on Recent Developments in Laboratory and Field Tests and Analysis of Geotechnical Problems*, Bangkok: 525-537.
- Randolph, M.F. 1986. RATZ-load transfer analysis of axially loaded piles. *Report GEO 86033*, Perth: Department of Civil Engineering, The University of Western Australia.
- Randolph, M.F. 1987. PIGLET, a computer program for the analysis and design of pile groups. *Report GEO 87036*, Perth: The University of Western Australia.
- Randolph, M.F. and Clancy, P. 1993. Efficient design of piled rafts. *Proc. of 2nd Int. Geot. Sem. on Deep Foundations on Bored and Auger Piles*, Ghent, 119-130.
- Randolph, M.F. and Wroth, C.P. 1978. Analysis of deformation of vertically loaded piles. *J. Geot. Eng. Div, ASCE* 104(12): 1465-1488.
- Randolph, M.F. and Wroth, C.P. 1979. An analysis of the vertical deformation of pile groups. *Geotechnique* 29(4): 423-439.
- Robertson, P.K. 1991. Estimation of foundation settlements in sand from CPT. *Proc. of Geotech. Eng. Congress*, Geotech. Eng. Div. ASCE, Boulder, Colorado, 764-775.
- Smith, D.M.A. and Randolph, M.F. 1990. Piled raft foundations - a case history. *Proc. Conf. on Deep Found. Practice*, Singapore, 237-245.
- Sommer, H. 1993. Development of locked stresses and negative shaft resistance at the piled raft foundation Messeturm Frankfurt/Main. *Proc. of 2nd Int. Geot. Sem. on Deep Foundations on Bored and Auger Piles*, Ghent, 347-349.
- Sommer, H., Tamaro, G. and DeBenedittis, C. 1991. Messe Turm, foundations for the tallest building in Europe. *Proc. 4th Int. Deep Found. Institute Conf.*, Sresa, 139-145.
- Thaher, M. and Jessberger, H.L. 1991. The behaviour of pile-raft foundations, investigated in centrifuge model tests. *Proc. Int. Conf. Centrifuge '91*, Boulder, Colorado, 225-234.
- Thorburn, S., Greenwood, D.A. and Fleming, W.G.K. (1993). The response of sands to the construction of continuous flight auger piles. *Proc. of 2nd Int. Geot. Sem. on Deep Foundations on Bored and Auger Piles*, Ghent, 429-443.
- Thorburn, S., Laird, C. and Randolph, M.F. 1983. Storage tanks founded on soft soils reinforced with driven piles. *Proc. Conf. on Recent Advances in Piling and Ground Treatment*, ICE, London: 157-164.
- Van Impe, W.F. 1991. Developments in pile design, *Proc. 4th Int. Conf on Piling and Deep Foundations*, Sresa.
- Van Impe, W.F. 1991. Deformations of deep foundations. *Proc. 10th Europ. Conf. on Soil Mech. and Found. Eng.*, Florence, 3, 1031-1062.
- Van Weele, A.F. 1993. Quality assessment foundation piles after installation. *Proc. of 2nd Int. Geot. Sem. on Deep Foundations on Bored and Auger Piles*, Ghent, 459-467.
- Vesic, A.S. 1969. Experiments with instrumented pile groups in sand. *Performance of Deep Foundations*, ASTM STP 444, 177-222.
- Viggiani, C. (1993). Further experiences with auger piles in Naples area. *Proc. of 2nd Int. Geot. Sem. on Deep Foundations on Bored and Auger Piles*, Ghent, 445-455.
- Viggiani, G. (1991). Dynamic measurement of small strain stiffness of fine grained soils in the triaxial apparatus. *Experimental Characterization and Modelling of Soils and Soft Rocks*, University of Naples, 75-97.
- Wroth, W.P., Randolph, M.F., Houlsby, G.T. and Fahey, M. 1979. A review of the engineering properties of soils, with particular reference to the shear modulus. *Cambridge University Research Report, CUED/D-Soils TR75*.
- Yamashita, K., Tomono, M. and Kakurai, M. 1987. A method for estimating immediate settlement of piles and pile groups. *Soils and Foundations* 27(1): 61-76.
- Yamashita, K., Kakurai, M., Yamada, T. and Kuwabara, F. 1993. Settlement behaviour of a five-storey building on a piled raft foundation. *Proc. of 2nd Int. Geot. Sem. on Deep Foundations on Bored and Auger Piles*, Ghent, 351-356.

ACKNOWLEDGEMENTS

The author acknowledges gratefully the input of ideas to this paper derived from discussions with many colleagues throughout the world, and would also like to thank Mr Patrick Clancy and Dr Martin Fahey, at the University of Western Australia, for their contributions in carrying out some of the analyses and in reviewing the paper. The assistance of Ms Vickie Byers in preparing many of the Figures and in final assembly of the paper is acknowledged with thanks.

NOTATION

| | |
|----------|---|
| a | radius of circular raft |
| A_g | total area covered by pile group |
| A_p | sum of cross-sectional areas of piles in group |
| B | width of rectangular raft |
| c_i | correction factors for pile group efficiency exponent |
| d | diameter of pile |
| d_{eq} | diameter of equivalent pier |

| | | | |
|-----------------|---|------------------|--|
| e | exponent in calculation of pile group efficiency | q _c | cone resistance |
| E _{eq} | Young's modulus of equivalent pier | Q _b | ultimate base capacity |
| E _p | Young's modulus of pile (assumed solid) | Q _s | ultimate shaft capacity |
| E _r | Young's modulus of raft or pile cap | Q _t | ultimate pile capacity |
| E _s | Young's modulus of soil | r _c | radius of pile cap (single pile) |
| f | parameter in modified hyperbolic stress-strain curves | r _m | maximum radius of influence of pile |
| F _D | embedment correction factor for raft settlement | r _o | pile radius |
| g | parameter in modified hyperbolic stress-strain curves | R | aspect ratio of pile group (equation (6)) |
| G | shear modulus of soil | R* | normalised radius of zone of modified soil |
| G* | normalised modified shear modulus adjacent to pile shaft | R _f | parameter in hyperbolic curve |
| G _b | shear modulus of soil below pile base | R _s | pile group settlement ratio |
| G _ℓ | shear modulus of soil at full penetration of pile shaft | s | centre-line spacing of piles |
| G _o | initial tangent shear modulus of soil | t | thickness of raft |
| h _i | thickness of soil layer | w _b | displacement of pile base |
| I _D | relative density | w _p | average displacement of pile group |
| I _e | influence factor for calculation of vertical strain | w _r | average displacement of raft |
| k _i | stiffness of i th foundation unit (load divided by settlement) | w _s | displacement of pile shaft |
| k _p | pile or pier stiffness (load divided by settlement) | w _t | displacement of pile top |
| k _{pr} | piled raft stiffness (load divided by settlement) | z | depth co-ordinate |
| k _r | raft stiffness (load divided by settlement) | | |
| K _o | at rest earth pressure coefficient | α _{ij} | interaction factor between foundation units i and j |
| K _{rc} | relative raft-soil stiffness ratio for circular rafts | α _{pr} | interaction factor between pile group and raft |
| K _{rs} | relative raft-soil stiffness ratio for rectangular rafts | α _{rp} | interaction factor between raft and pile group |
| ℓ | embedded length of pile | Δ | increment |
| L | length of rectangular raft | ζ | load transfer parameter for pile shaft |
| m | parameter in parabolic load transfer curves | η | pile group efficiency; ratio of pile base radius to shaft radius |
| M _s | shaft flexibility parameter in CEMSET | λ | pile-soil stiffness ratio, E _p /G _ℓ |
| n | number of piles in group | μ | parameter in solution for single pile response |
| N | SPT blow-count | ν | Poisson's ratio of soil |
| OCR | overconsolidation ratio | ξ | parameter for pile base flexibility |
| p' | mean effective stress | π | mathematical constant |
| p _a | atmospheric pressure (100 kPa) | ρ | parameter for relative homogeneity of soil modulus |
| P _b | base load for single pile | σ' _{vo} | vertical effective stress |
| P _p | load carried by pile group | τ | shear stress |
| P _s | shaft load for single pile | τ _φ | failure shear stress |
| P _t | total load at pile head | τ _o | shear stress at pile-soil interface |
| q | applied pressure | τ _s | limiting shaft friction |
| q _b | end-bearing pressure | ψ | parameter in non-linear load transfer response of pile shaft |